

---

# Uncovering interpretable potential confounders in electronic medical records

---

Jiaming Zeng<sup>1</sup>, Michael F. Gensheimer<sup>2</sup>, Daniel L. Rubin<sup>3</sup>, Susan Athey<sup>4</sup>, and Ross  
D. Shachter<sup>1</sup>

<sup>1</sup>Department of Management Science and Engineering, Stanford University

<sup>2</sup>Department of Radiation Oncology, Stanford School of Medicine

<sup>3</sup>Department of Biomedical Data Science, Radiology, and Medicine, Stanford  
School of Medicine

<sup>4</sup>Graduate School of Business, Stanford University

February 1, 2022

## Abstract

Randomized clinical trials (RCT) are the gold standard for informing treatment decisions. Observational studies are often plagued by selection bias, and expert-selected covariates may insufficiently adjust for confounding. We explore how unstructured clinical text can be used to reduce selection bias and improve medical practice. We develop a framework based on natural language processing to uncover interpretable potential confounders from text. We validate our method by comparing the estimated hazard ratio (HR) with and without the confounders against established RCTs. We apply our method to four cohorts built from localized prostate and lung cancer datasets from the Stanford Cancer Institute and show that our method shifts the HR estimate towards the RCT results. The uncovered terms can also be interpreted by oncologists for clinical insights. We present this proof-of-concept study to enable more credible causal inference using observational data, uncover meaningful insights from clinical text, and inform high-stakes medical decisions.

---

\*email: [jiaming@alumni.stanford.edu](mailto:jiaming@alumni.stanford.edu)

## 1 Introduction

As the number of highly targeted cancer treatments increase, it is increasingly difficult for oncologists to decide on optimal treatment practices. In the recent years, medicine has seen the reversal of 146 standard medical practices [1], and many unanswered questions remain on treatment decisions in oncology. The gold standard for assessing treatment effects is randomized clinical trials (RCT). However, RCTs can be very expensive, time-consuming, and limited by the lack of external validity [2, 3]. Hence, there has been a growing interest in using observational data to compare and evaluate the effectiveness of clinical interventions, also known as comparative effectiveness research (CER) [2].

Many studies have used large-scale observational registries such as the Surveillance, Epidemiology, and Ends Results (SEER) and National Cancer Data Base (NCDB) to perform CER. However, such studies may be unreliable due to the systemic bias present in observational data and the presence of unmeasured confounders [1, 2, 4]. Moreover, population-based CERs in oncology often also face small data challenges. Electronic medical records (EMRs) are another source of rich observational information on patient demographics and past medical history. We hypothesize that the more detailed unstructured data present in EMRs can be harnessed to reduce confounding compared to prior CER studies.

In the past decade, there has been a growing interest in using observational data for clinical decision making and causal inference in oncology [2]. However, such studies are often unreliable, and many observational studies have been refuted by RCTs soon after [2, 4]. For example, Yeh et al. [5] performed a comparison of surgery vs. radiotherapy for oropharynx cancer and suggested that surgery may be superior to radiation for quality of life outcomes. A few years later, this claim was refuted by an RCT study Nichols et al. [6], which showed that radiation is in fact superior to surgery in terms of 1-year quality of life scores. A similar example is seen with prostate cancer. In 2016, Wallis et al. [7]

showed through population-based studies that surgery is superior to radiation for early-stage prostate cancer for overall and prostate cancer specific survival; a few months later, the finding was refuted by Hamdy et al. [8], which showed that surgery and radiation are equivalent in terms of overall and prostate cancer specific survival. Many other studies have shown the fallibility of population CERs that rely on expert-curated features to draw conclusions about treatment effects [2][9].

Beyond clinical studies, there is a relatively large literature on performing causal inference from observational data. Various papers have explored how to correct for bias when evaluating average treatment effect (ATE) from observational studies with propensity score matching or weighting [10][11]; see [12] for a review. There is also a growing amount of literature that adapts machine learning models, such as random forest or regularized regression, for doubly-robust ATE estimation in high-dimensional settings [13][14][15][16]. However, most of the methods do not include unstructured data.

Recent literature has shown the usefulness of conditioning on textual data to adjust for confounding [17][18][19][20]. Roberts et al. [18] proposes text matching to employ textual data for causal inference. Mozer et al. [17] applies text matching to patient charts texts for a medical procedure evaluation; however, they focus on continuous outcomes and rely mostly on expert-curated terms from the clinical text. Veitch et al. [19] is another work that employs unstructured data for causal inference; however, they rely on black-box models that are not interpretable. Moreover, many existing causal inference methods are developed for continuous outcomes and do not transfer easily to the time-to-event outcomes for survival analysis used in oncology. Of the ones that perform causal inference on time-to-event outcomes for medical applications [21][22], we did not find any that include unstructured data in a systematic way. Austin [22] presents methods for using propensity scores to reduce bias in observational studies with time-to-event outcomes. Our study

leverages some of the ideas and methods in this literature to develop our approach for identifying and evaluating the potential confounders from the unstructured clinical notes. Keith et al. [20] presents a review of the literature on using textual data to adjust for confounding. Our paper contributes to this literature by addressing obstacles in using NLP methods to remove confounding.

There is also a growing literature that seeks to better employ EMRs for clinical tasks. Existing work has employed structured EMR data and unstructured clinical notes for survival prediction and analysis [23 24], clinical risk prediction [25], and prediction of multiple medical events [26]. However, most current work involving EMRs focuses on prediction tasks. In studies that include the unstructured notes, most use deep learning to produce context-rich embedding representations of words or documents [23 26]. While these representations are highly accurate for prediction tasks, they are often black-box and very difficult to interpret for causal insights. Our approach differs in that we use simple NLP techniques (e.g. entity identification, bag-of-words) to generate matrix representations that can be easily mapped to specific words and phrases. This increases the interpretability of our method and allows us to explain our confounders to clinicians.

We study how EMRs, especially clinical text, can be used to reduce selection bias in observational CER studies and better inform treatment decisions in oncology. A confounder is a variable that is associated with both treatment assignment and the potential outcomes a subject would have under different treatment regimes. In the presence of confounders, the correlation between treatment assignment and outcomes cannot be interpreted as causal. One way that confounding may arise is when patients are selected for a treatment group on the basis of the severity of their illness. In such a case, failing to adjust for patient severity can lead to selection bias when attempting to estimate causal effects. For example, surgery tends to be performed on younger or healthier patients; certain doctors or

institutions may prefer one treatment over another, and this creates confounding if those doctors or institutions treat patients with systematically different severity. Studies based on a small set of covariates tend not to capture the important confounders and result in biased estimates [7, 5]. Observational studies are more reliable when we can better control for these confounders. While structured EMR data, such as billing codes, can be used to encode expert-curated patient characteristics, studies suggest that administrative claims data may contain errors [27, 28] and expert-curated covariates may not capture all potential confounding [7, 29]. EMR clinical text is a potential source of additional information about factors that might relate to both treatment assignment and prognosis.

We propose an automated approach using natural language processing (NLP) to uncover interpretable potential confounders from the EMRs for treatment decisions. For high-stake settings such as cancer treatment decisions, it is important to design models that are interpretable for trust and understanding [30]. NLP can be used to process the unstructured clinical notes and create covariates that supplement the traditional covariates identified through expert opinion. We then augment our dataset with covariates that impact both treatment assignment and patient outcomes, where attempting to estimate causal effects while omitting such variables leads to biased estimates [31, 15]. Finally, we use methods designed to estimate causal effects in observational studies with observed confounders to estimate treatment effects in our augmented data set. We show that controlling for these confounders appears to reduce selection bias when compared against the results from established RCTs and clinical judgement.

We apply our method to localized prostate and lung cancer patients. Based on cohorts from established RCTs, we built four treatment groups for comparison. We uncovered interpretable potential confounders from clinical text and validated the potential confounders against the results from the RCTs. Simple NLP techniques (e.g. lemmatization, entity

identification) were used to construct a bag-of-words representation of the frequently occurring terms. A Lasso model [32] was then used to select the terms that are predictive of both the treatment and survival outcome as potential confounders. Finally, we validated our method by comparing the hazard ratio (HR) from survival analysis with and without the confounders.

Our main contribution is presenting a framework for uncovering interpretable potential confounders from clinical text. Existing work in observational causal inference rarely employs unstructured data [11, 21, 22], and most NLP studies on clinical text focus on prediction or classification settings [23, 26, 28]. Our paper differs from existing studies by employing NLP for causal analysis; we use NLP methods to predict the treatment and survival outcome, and then employ a causal framework to combine the two models for uncovering potential confounders. We are the first to uncover interpretable potential confounders from clinical notes for causal analysis on cancer therapies, and one of the few works that combines NLP and causal inference in a time-to-event setting. Our method allows researchers to extract and control for confounders that are not typically available. While we present our work as a proof-of-concept study, this appears to be a useful step for future observational CER studies to help reduce selection bias unique to that dataset. The research presented can help unlock the potential of clinical notes to help clinicians understand current clinical practice and support future medical decisions. We also outline several limitations that need to be overcome for use in practice in Section 3.

Our study advances both the clinical and causal inference literature by using NLP to perform causal inference on clinical text in time-to-event settings. We hope this will inform clinical practice and improve patient outcomes.

## 2 Results

We apply our methods to localized prostate and stage I non-small cell lung cancer (NSCLC) patients and compare the results against established RCTs. We select these diseases due to data availability and having established clinical RCTs for validation. After filtering and assignment, we include 1,822 patients for prostate cancer, with 988 surgery patients, 385 radiation patients, and 449 active monitoring patients; the average follow-up time is 4.11 years. For stage I NSCLC, we include 749 patients, with 492 surgery patients and 257 radiation patients; the average follow-up time is 4.96 years. The patient characteristic descriptions of the prostate cancer cohort are shown in Table 1 and the NSCLC cohort are shown in Table 2. Please see Section 4.1 for more details on the patient selection process.

We use the findings from established RCTs and clinical judgement as a benchmark for evaluating our results. For localized prostate cancer, Hamdy et al. [8] compared active monitoring, radical prostatectomy, and external-beam radiotherapy. A total of 1,643 patients were included in the study, with 553 men assigned to surgery, 545 men assigned to radiotherapy, and 545 men to active monitoring. They observed no significant difference among the groups for prostate cancer or all-cause mortality ( $P = 0.48$  and  $P = 0.87$  respectively). Similarly, a recent study showed that difference in treatment effects for surgery vs. radiation observed from observational studies is entirely due to treatment selection bias [29]. For stage I NSCLC, the Chang et al. [33] study is a pooled study comparing stereotactic ablative radiotherapy (SABR) to surgery. A total of 58 patients were included, with 31 patients assigned to SABR and 27 to surgery. The study observed that SABR had slightly better overall survival than surgery ( $P = 0.037$ ), but claims to be consistent with the clinical judgement that surgery is equipoise to radiation.

Following the design of Hamdy et al. [8] and Chang et al. [33], we evaluate our results for the following four treatment groups for an outcome of all-cause mortality:

- surgery vs. radiation for prostate cancer
- surgery vs. monitoring for prostate cancer
- radiation vs. monitoring for prostate cancer
- surgery vs. radiation for stage I NSCLC

We do not analyze other treatment groups for lung cancer due to patient count constraints.

Our approach identifies covariates that are likely potential confounders in this particular dataset from the high-dimensional and high-noise EMR data. These covariates are interpretable as they are represented by structured data or words from a bag-of-words matrix. To evaluate the effectiveness of the potential confounders selected in the model, we use these potential confounders to perform survival analysis for the treatment groups for prostate and stage I NSCLC. We compare the results of various methods for time-to-event analysis in terms of HR. Although we cannot know what the true HR is, we suggest that using medical notes improves on the traditional covariates. We compare our results against existing RCTs to evaluate how the confounders we have uncovered can help correct for selection bias. The overall workflow is shown in Figure [1](#). Supplement [1](#) details the covariates extracted from the structured data.

## 2.1 Potential Confounders

We show that our methods uncover terms that are predictive of both the treatment and survival outcome. Hence, these are potential confounders that should be controlled for in observational CERs to reduce selection bias. Please see Supplement [3](#) for a discussion on the structures of potential confounding our method can capture.

We select the intersection covariates from our treatment and outcome prediction models as the potential confounders. We base this idea on the selection of union variables to



reduce confounding when performing causal inference on observational data in the case of continuous outcomes [15]. However, in survival analysis, it is recommended that the covariates analyzed be constrained by the statistical 1 in 10/20 rule of thumb with respect to the event count [34, 35]. In our high-dimensional setting, the union of covariates that are predictive of treatment and outcome yield too many potential confounders relative to the sample size. Hence, we use the intersect as a heuristic to focus on the most important confounders.

In Figure 2 we illustrate the unpenalized coefficients of covariates from two models, the treatment assignment model and the survival outcome model. For each covariate, the  $x$ -axis plots the coefficient from the treatment prediction model while the  $y$ -axis plots the coefficient from the survival outcome model. Each covariate is labeled by the text next to it. The intersection covariates, *intersect*, are shown in blue; these are the covariates that have strong effects in both models. For the structured covariates, we illustrate in black the coefficients for the covariates that were not selected; these coefficients are closer to at least one of the axes in the figure. We do not illustrate the coefficients for unstructured covariates that are not selected, as there are a large number of these covariates. The axes are labeled to indicate which treatment the coefficient predicts and whether the coefficient is indicative of a good or bad survival prognosis. For example, in the treatment model, patients with a high bladder word-occurrence have a higher likelihood of receiving surgery; in the outcome model, patients with a high bladder occurrence have a lower likelihood of survival.

In Supplement 5, we show the  $R^2$  correlation among all the selected covariates for each treatment group.

## 2.2 Evaluation of Potential Confounders

We evaluate these potential confounders by comparing the results on 3 covariate combinations:

- **structured**: Using only the structured covariates. We use this as a baseline because these are covariates that are typically used in retrospective oncology studies and are readily available in the structured data [7].
- **intersect**: Using only the intersection covariates identified as confounders.
- **struct+intersect**: Using the union of the structured and intersection variables.

We then perform survival analysis using univariate Cox proportional hazard models (Cox-PH) with propensity score matching (**matching**), univariate Cox-PH model with inverse propensity score weighting (**IPTW**), and multivariate Cox-PH model with inverse propensity score weighting (**multi.coxph**). We hypothesize that **struct+intersect** will perform the best by including both the structured and unstructured data. In Figure 3 we show the hazard ratio (HR) of the effect of treatment for each study cohort when the selected covariates are included in analysis. An HR below 1 indicates that patients with the second treatment are more likely to survive than those with the first treatments. An HR above 1 indicates the opposite, and an HR equal to 1 indicates that the two treatments are equipose. For each HR estimate, we also show the 95% confidence interval (CI). Please see Section 4.5 for more details on the methods.

We observe that with the additional covariates, we are able to shift the estimate of the HR towards the direction of the RCT for an outcome of all-cause mortality. We also compare the covariate-specific HR of each of the selected covariates in terms of univariate and multivariate Cox-PH analysis for an all-cause mortality outcome in Tables 3-6.

In Figure 3a and Table 3 we show the results with surgery vs. radiation for prostate cancer. The RCT reports no significant difference between surgery vs. radiation for localized prostate cancer 8. With `structured`, we observe a significant effect that radiation is superior to surgery, a result that disagrees with most retrospective studies 7. Each center can have different patient populations and treatment patterns that shift the only structured adjusted survival rates. For instance, at our center we have a busy high-dose-rate brachytherapy program which is an attractive option for fit patients with few comorbidities who might otherwise receive surgery. This would be expected to bias the survival outcomes in favor of radiation, as observed in our study. We seek to uncover potential confounders from the text that can reduce bias when performing retrospective studies, whichever way the bias lies. After adjustment with the uncovered confounders, we observe a significant shift in the HR towards equipose with the additional identified confounders for `intersect` and `struct+intersect`. For `structured`, we observe an HR of 2.51 with 95% CI (2.39-4.55) and  $p$ -value of 0.002 with `multi.coxph`. For `struct+intersect`, we estimate an HR of 1.54 with 95% CI (0.78-3.03) and  $p$ -value of 0.214 with `multi.coxph`. We shift the HR point estimate by 0.97, or 38.6%, towards equipose.

In Figure 3b and Table 4 we show the results of surgery vs. active monitoring for prostate cancer. Hamdy et al. 8, the RCT, reports the HR for surgery vs. active monitoring as 0.93 with 95% CI (0.65, 1.35) and  $p$ -value of 0.92. With `structured`, we again have a significant effect that active monitoring is superior to surgery; this disagrees with most retrospective studies 7 and Hamdy et al. 8. We again observe a significant shift in the HR towards equipose with the additional identified confounders. For `structured`, we observe an HR of 2.71 with 95% CI (1.55-4.75) and  $p$ -value  $< 0.001$  with `multi.coxph`. For `struct+intersect`, we estimate an HR of 1.10 with 95% CI (0.55-2.21) and  $p$ -value of 0.781 with `multi.coxph`. We shift the HR point estimate by 1.61, or 59.1%, towards equipose.

In Figure 3c and Table 5 we show the results of radiation vs. active monitoring for prostate cancer. We do not see as significant a shift with radiation vs. active monitoring. Hamdy et al. [8] records the HR for radiation vs. active monitoring as 0.94 with 95% CI of (0.65, 1.36) and  $p$ -value of 0.92. We observe that **matching** estimated the HR closest to the RCT results when compared against **IPTW** and **multi.coxph**. All results with **intersect** and **struct+intersect** shift the HR estimate slightly towards equipose, with the most shift of 0.32, or 71.1%, by **intersect** and **IPTW**; this is closely followed by a shift of 0.20, or 45.5%, with **intersect** and **multi.coxph**. While the adjusted results are not as close to the RCT results as compared to Figures 3a-b, the HR estimate are all shifted towards the RCT results in terms of bias reduction for each of the data and method combination. We suspect the less significant shift may be due to the smaller dataset available for radiation vs. active monitoring or the confounding not being observable within the text.

In Figure 3d and Table 6 we show the results with surgery vs. radiation for stage I NSCLC. With **structured**, we observe a significant effect that surgery is superior to radiation. The results from Chang et al. [33] and clinical judgement tells us that surgery and radiation should be about equipose for stage I NSCLC. The shift is not as significant as with prostate cancer, but we also note that the established clinical standard for lung cancer is not as well studied. We observe a more significant shift with **multi.coxph**, with an average shift of 0.15 or 38.5%. We observe an average shift of 0.06, or 15.4%, with **matching** and an average shift of 0.02, or 5.1% with **IPTW**. For **structured**, we observe an HR of 0.39 with 95% CI (0.30-0.51) and  $p$ -value  $< 0.001$  with **multi.coxph**. For **struct+intersect**, we estimate an HR of 0.54 with 95% CI (0.40-0.53) and  $p$ -value  $< 0.001$  with **multi.coxph**. We shift the HR point estimate by 0.15, or 38.5%, towards equipose. While the adjusted results are not as close to the RCT results as compared to Figures 3a-b, the HR estimates are all shifted towards equipose in terms of bias reduction for each combination. We suspect

the less significant shift is again due to the even smaller data size of stage I NSCLC. The doubly-robust method of `multi.coxph` seem to perform better under these settings.

Overall, our methods uncover several potential confounders that can reduce selection bias in observational data. Although our method cannot uncover all potential confounders, we are able to uncover confounders that are not usually included in expert-selected covariates. Supplementary analysis of propensity scores and covariate balance plots for each analysis is seen in Supplement [4](#).

### 2.3 Potential Confounder Interpretation

We show that the potential confounders we have uncovered are interpretable through clinical expertise. We examine the effect on survival for each selected covariate in term of univariate and multivariate survival analysis with a Cox-PH model. In univariate analysis, a single covariate is regressed on the survival outcome and describes the survival with respect to a single covariate. In multivariate analysis, all the selected covariates are regressed on the survival outcome and describe each covariate's effect on survival while adjusting for the impact of all selected covariates. For a particular variable, an HR below 1 indicates that the covariate is a positive predictor of survival, an HR above 1 indicates a negative predictor of survival, and an HR equal to 1 means that the variable does not seem to effect survival.

For surgery vs. radiation and surgery vs. active monitoring with prostate cancer, `struct:patient.age`, `text:bladder`, and `text:urothelial` are chosen as intersection covariates. Moreover, they are also shown to be significant through both univariate and multivariate covariate analysis in Tables [3](#) and [4](#)

Patient age is a known confounder in treatment decision and survival outcomes. Older patients are more likely to receive radiation due to surgery risk. However, older pa-

tients also have higher mortality. In Figure 2a-c, we observe that patients with higher `struct:patient_age`, i.e. older patients, are more likely to receive radiation and a bad prognosis.

We hypothesize that `text:bladder` and `text:urothelial` are identified because prostate cancer patients often have bladder symptom issues and can also have urothelial cancer. Most retrospective prostate cancer studies have not excluded patients with early stage bladder cancer [7]. Examples of `text:bladder` in the clinical notes are “he notes incomplete bladder emptying”, “evidence of benign prostatic hyperplasia and chronic bladder outlet obstruction”, and “diagnosis of bladder cancer”. Examples of `text:urothelial` in the notes are “pathology showed high grade urothelial carcinoma with muscle present and not definitively involved”, “it was read as a high grade urothelial cancer which involved the stroma of the prostate as well as the bladder”. Patients with bladder cancer or bladder issues are more likely to get surgery than radiation. Radiation does not work well for bladder cancer. Patients with bladder problems may prefer surgery because radiation can irritate the bladder and cause urinary problems. However, these are also patients with higher mortality and more health issues. In Figure 2a-b, we observe that `text:bladder` and `text:urothelial` are more common in patients who received surgery and had a bad prognosis.

Moreover, for this dataset, we note that the confounding appears to be observable. The bias of surgery being worse than radiation and monitoring is due to a group of patients who are diagnosed with prostate cancer through a resection for bladder cancer or other bladder issues. When a patient with bladder cancer has a cystoprostatectomy in which the bladder and prostate are both removed, a pathologist can sometimes find a prostate tumor in the pathology specimen. Bladder cancer patients tend to be older, have more medical issues, and a higher mortality rate. The terms `text:bladder` and `text:urothelial` describe this group of patients. Our method can capture some characteristics of this group and use

this to reduce selection bias.

For radiation vs. active monitoring, we do not observe confounders that present a significant shift in treatment HR in Table 5. It can be that the confounding here is not as easily observable or our method is unable to identify it. We can identify interesting potential confounders, such as text:resident. From Figure 2, we observe that text:resident is more common in patients who received radiation and had a bad prognosis. This term likely refers to both resident physicians and the patient being a resident of a long-term care facility or skilled nursing facility. Both uses of the term could reduce survival time: inpatients at teaching hospitals have much of their care delivered by resident physicians, and frequent inpatient stays or nursing facility residency could both indicate a sicker patient.

We repeat the same process for lung cancer. We examine Table 6 for the intersection covariates through univariate and multivariate analysis. We observe that some of the significant terms are struct:patient\_age, struct:male, struct:race\_api, struct:diagnosis\_year, text:alk, text:left.low, and text:severe.

We note that age, gender, race, and diagnosis year are known confounders for treatment decision and outcome.

The covariate text:alk points to the ALK mutation for NSCLC. About 5% of NSCLCs have a rearrangement in a gene called ALK; the ALK gene rearrangement produces an abnormal ALK protein that causes the cells to grow and spread. This change is often seen in non-smokers (or light smokers) who are younger and who have the adenocarcinoma subtype of NSCLC 36. It's been observed that patients with the ALK mutation have worse disease-free survival, citing higher rates of recurrence and metastasis 36. Alternatively, we hypothesize that text:alk is significant because the ALK mutation is mutually exclusive from the EGFR mutation 37. The EGFR mutation is often present in asian patients and EGFR patients typically have better survival. Hence, the significance of text:alk can be

related to the absence of the EGFR mutation. In Figure 2d, we observe that text:alk is more common in patients who received radiation and had a bad prognosis.

The covariate text:left.low can point to NSCLC on the lower left node of the lung. Studies have observed that lung cancer on the lower lobe or lower left lobe has worse survival [38, 39]. This can also be related to the absence of the EGFR mutation, since EGFR mutation occur less frequently in the lower lobe [38]. In Figure 2d, we observe that text:left.low is also more common in patients who received radiation and had a bad prognosis.

The covariate text:nipple can indicate a history of breast cancer. Studies have shown that patients with a history of breast cancer are diagnosed with lower stages of NSCLC and show better prognosis when compared to women with first NSCLC, perhaps due to heightened surveillance compared to the general population [40]. In Figure 2d, we observe that text:nipple is more common in patients who received surgery and had a good prognosis; both effects have also been observed in Milano et al. [40].

The covariate text:sponge can refer to sponges used for surgical preparations. Sponge is commonly used in surgery and can be an indication that the patient has some history of receiving surgery. Patients who receive surgery tend to be healthier and have better survival. In Figure 2d, text:sponge is more common in patients who received surgery and had a good prognosis.

The covariates text:severe and text:rib could be pointing to a severe conditions related to lung and other problems that indicate poor overall health and performance status, which has been shown to be related to a patient's survival outcomes [41]. Examples of text:severe include phrases such as “severe pulmonary hypertension”, “severe COPD”, or “severe emphysema”. Examples of text:rib include phrases such as “rib fractures” or “rib shadows”. In Figure 2d, we observe that both text:severe and text:rib are more common in



patients who received radiation and had a bad prognosis. Similarly, we also observe other terms that could describe the type of lung cancer - such as `text:squamous.cell` - or overall health levels - `textdstext:alert`, `text:attention`.

Overall, we are able to uncover some potential confounders that are easy to interpret and capture useful clinical insights.

### 3 Discussion

We have demonstrated how causal inference methods can be used to draw more reliable conclusions from population-based studies. Our paper shows that 1) clinical notes, or unstructured data, can be an important source for uncovering confounders, and 2) current clinical tools can be augmented with machine learning methods to provide better decision support. Furthermore, our proof-of-concept framework can be easily adapted to use textual data to reduce selection bias in retrospective studies more generally.

Our framework can be used to improve clinical practice. Due to the simplicity of the machine learning tools employed, it can be easily implemented as an additional step in the design of observational CER studies. Our results also show that the method is generalizable to different types of cancer and for various types of study cohort comparisons. With the continued digitization of clinical notes and the increasing access to EMRs, we recommend this as an essential step for any researcher seeking to draw clinical insights from observational data. The terms uncovered with our method can not only be used to improve observational CERs, but also be used to generate interpretable insights about current clinical practice. The uncovering of relevant information and subsequent insights can then be used to inform high-stakes medical decisions.

We believe that our work is the first to explore the potential of including unstructured clinical notes to reduce selection bias in oncology settings. We are also one of the first

works to incorporate unstructured data into causal inference estimators and Cox-PH models. Although our method has been developed to address a specific problem in oncology and applied in the clinical setting, it can also be easily adapted for application in any observational study that seeks to incorporate unstructured text. We propose our method as an automated selection procedure that can be used to supplement expert opinion when uncovering potential confounders for a particular observational study population. There is much work to be done in using NLP and unstructured text for causal inference. Our work presents a simple and flexible way to generate interpretable causal insights from text of any sort. Our method can also be applied to studies within and beyond medicine to extract important information from observational data to support decisions.

Our study also has several limitations. We begin by outlining potential areas for future work. First, we use simple NLP methods to process the clinical notes and extract the top 500 or 1000 features for variable selection. In the process, much information in the text nodes are discarded and the sequence of past medical events are not taken into account. We choose this setup due to the small sample size of oncology study cohorts, which makes it difficult to train more complicated models for textual processing. In theory, the more work that is placed into the clinical notes preprocessing and the higher quality of the features generated from these notes, the more informative the uncovered potential confounders will be. For future work, we hope to explore how other NLP techniques, such as topic modeling or clustering, can be used to build even higher quality features from the unstructured text. There are also an increasing number of deep learning models that can be used to identify interpretable insights [26]. We are interested in how these deep learning methods can be applied to generate causal insights on another study population with larger sample size. We are also interested in developing ways to better address ambiguity in the notes (e.g. “it is unclear if the patient has chest pain”).

Second, we rely on the proportional hazard assumption for our Cox-PH models. In cases of many covariates, the assumption may be violated. We feel the simplicity and interpretability of the model outweigh the performance improvement resulting from increased complexity. For EMR datasets with many covariates, the assumption is often used and does not seem to present a practical issue [24]. Future work could explore alternative models that do not rely on the assumption [42].

Third, more work can be done to mitigate immortal time bias in our HR estimates. We discuss our approach in Section 4.2. An alternative method to address this problem would be to use a time-dependent Cox-PH model [43].

Fourth, we focus on comparison of methods that can be applied in a time-to-event setting, and leave out more novel methods that are developed for continuous settings of ATE estimation. It would be interesting to explore how these methods can be extended and applied to a time-to-event setting.

Fifth, our approach of selecting intersection covariates is an empirical approach designed for uncovering the most valuable potential confounders. As a result, we filtered out most of the features and only focused on a few confounders. While our approach works well empirically in this study, future work involves developing more sensitive and statistically grounded methods for identifying potential confounders.

Sixth, our work is constrained to localized prostate and lung patients at the Stanford Hospital and state cancer registry data. It would strengthen the validity of our methods if experiments can be performed on large multi-institutional registries for cancer or other diseases.

Seventh, we acknowledge that an average follow-up of about 4 years is relatively short for prostate cancer survival analysis. For this sample from the EMR, the actual follow-up time for each patient varies from 6-months to 10 years. Future studies can perform the

analysis on larger multi-institutional datasets.

Eighth, we include a limited set of structured features as structured data such as diagnosis codes are often under-reported in the EMR. For example, we did not include the PSA scores because they are not well recorded in the structured data as many patients had PSA tests done at outside facilities [44]. We do include tumor grade in the structured data, which is shown to have a strong correlation to PSA [45]. We acknowledge this as a limitation of our study and future work can be done to augment the structured features.

In addition to future works, we also outline two limitations to applying our framework. First, our method can only uncover potential confounders that can be observed in notes. There are many sources of confounding in observational data and even rich EMR data cannot capture everything. If the confounding is unknown and unobservable, no method to our knowledge will be able to adjust for it. Hence, it would be good practice to perform sensitivity analysis to evaluate the result's robustness to unknown confounding. Please see Supplement 3 for additional discussion on the potential confounding situations we can capture.

Second, the validity of causal inference models cannot be determined without prospective experimental data. Therefore, the uncovered confounders and estimated HR can only be validated by clinicians. We are identifying potential candidates for the bias and then evaluating these candidates of bias against RCTs.

Many challenges remain for employing unstructured data for causal inference analysis and medical settings. We hope this work interests both clinical practitioners augmenting existing clinical support tools and researchers using textual data to reduce confounding in observational data. We hope our workflow, problem framing, and experimental design can serve as such a sandbox for testing more complex algorithms or adapting to other application areas. Ultimately, we hope this research will find causal information in clinical notes

and provide a transparent way for machine learning to inform medical decision making.

## 4 Methods

### 4.1 Dataset

Our research conforms with all relevant ethical regulations and is approved by the Stanford Institutional Review Board (IRB). Patient consent was waived through obtaining the IRB. We curate a dataset of non-metastatic prostate and lung cancer patients from the Stanford Cancer Institute Research Database (SCIRDB). The database includes patients seen in the Stanford Health Care (SHC) system from 2008 to 2019 for prostate cancer and 2000 to 2019 for lung cancer. SHC clinical sites include one academic hospital, one freestanding cancer center, and several outpatient clinics. From SCIRDB, we pull a total of 3,638 prostate cancer patients with 552,009 clinical notes and 3,274 non-small cell lung cancer (NSCLC) patients with 648,505 clinical notes. The clinical notes include progress notes, letters, discharge summaries, emergency department notes, history and physical notes, and treatment planning notes.

For each patient, we also pull the structured EMR and data from the inpatient billing system. From the California Cancer Registry (CCR), we pull the available initial treatment information, cancer staging, tumor description, date of diagnosis, date of death, and date of last follow-up for these selected patients. For NSCLC, we also pull the recorded Epic cancer staging information. Demographic information such as age, race, gender, and ethnicity are self-reported in our dataset.

## 4.2 Study Cohort

We build our study cohorts from SCIRDB with reference to existing observational study principles and clinical expertise. We try our best to select patients for each treatment group built from the EMRs to match the RCTs criteria.

For each patient, we combine all treatments with the same Diagnosis ID in the CCR as the initial line of treatment. For patients with multiple Diagnosis ID, we keep the first record of treatment. For prostate cancer, patients without a recorded treatment are labeled as active monitoring. To avoid explicit revelation of the treatment choice, we only include notes more than 2 months before treatment start date for prostate cancer and 1 month for NSCLC. We rely on domain expertise to determine the 1 or 2-month pre-treatment cutoffs. Lung cancer patients typically have higher mortality and tend to start treatment pretty quickly. For prostate cancer, patients progress more slowly and get second opinions before making a treatment decision. We then select for patients with at least one note before the specified time. We select only patients who survived at least 6 months past their date of diagnosis to mitigate immortal-time bias [43]. We then filter for only patients with treatment of interest for analysis. Because we extract only initial treatments (rather than treatments for cancer recurrence) as recorded in SEER, most of the treatments are administered within 6 months of the diagnosis date [46]. This is similar to the setup for traditional landmark analysis [43]. To ensure the proportional hazard condition, patients who are still living are censored at time of last follow-up [47]. The patient filtering and cohort selection process is shown in Figure 4.

For patients with unknown clinical stage but known pathological stage, we impute the clinical stage by training a clinical stage classification model using the pathological stage and other patient information. Pathological stage is usually a little higher than clinical stage due to the staging based on biopsy samples instead of imaging; hence, it is inaccurate

to group them together. Clinical stage is more frequently used for similar observational studies [8, 33] and it is more rigorous to impute the missing clinical stage with a model trained on the pathological stage and other relevant covariates. We train the clinical stage imputation model with `struct:patient_age`, `struct:pathological_stage`, `struct:diagnosis_year`, and `struct:tumor_grade`. For NSCLC, `text:tumor_grade` is not included due to missing information. For both prostate and NSCLC, we train and validate a random forest model [48, 49] on patients with both clinical and pathological stage available. The imputed stages are used as the clinical stage for those patients. For patients with both clinical and pathological stage missing, we are able to fill in some through clinical chart reviews.

We assign patients to the treatment groups based on the initial treatment decision to capture the intent to treat rather than the actual treatments administered. We assign patients with only surgery records into the surgery group and patients with only radiation records into the radiation group. For patients with both radiation and surgery, patients who received surgery first are assigned to the surgery group and patients who received radiation first to the radiation group. For prostate cancer, patients from all stages are included, except for patients with distant metastases, and patients with no recorded treatment are assigned to the active monitoring group. For NSCLC, only patients with clinical stage I are included. The data processing is performed in python with pandas [50].

### 4.3 Data Processing and Representation

We build the covariates used for uncovering confounders through the process shown in Figure 1A. We compile the data from SCIRDB, CCR, and Epic for each patient.

We include age, race, ethnicity, clinical stage, and diagnosis year as part of the structured data. For prostate cancer, we also include SEER-recorded tumor grade, which are highly correlated with the Gleason grade. For NSCLC, we also include gender. Based on

age range categories used in Li et al. [51], we form the categorical variable `struct:patient_age` by splitting age into ranges of  $\leq 49$  years-old, 5-year buckets from 50 – 84 years-old, and  $\geq 85$  years-old. Race and ethnicity are encoded as one-hot vectors, with each feature indicating one race or ethnicity. Race is combined based on what is done in Li et al. [51]. We select these structured covariates because they are commonly accepted by clinicians as potential confounders and often included in CER studies [7]. For race, `struct:race_unknown` is not included as a covariate. For ethnicity, only `struct:hispanic` is included as a covariate. For tumor grade, patients with unknown grade are imputed with the median grade value. The indicator variable `struct:grade_unknown` is added to indicate which patients have been imputed. The covariates `struct:tumor_grade` and `struct:grade_unknown` are not included for NSCLC due to missing information of tumor grade and clinical judgement. In the end, we have 9 structured covariates for prostate cancer and 7 structured covariates for NSCLC. While billing codes can be used to generate additional structured features for diagnosis and past treatments, existing studies have found these can be unreliable [27] [28]. Hence, we chose to focus mainly on clinical notes to capture additional information that can influence survival time, such as patient symptoms and performance status.

We build word frequency representations of the clinical notes for the unstructured covariates. For each patient, we compile notes within the specified time (i.e. 2 months prior to treatment start date for prostate cancer and 1 month prior for NSCLC). We only use notes from before treatment so that we are not predicting survival outcome with information unavailable at the time of treatment decision. The different time windows for the two diseases were selected as NSCLC treatment generally starts more quickly than prostate cancer treatment due to the more rapidly progressing nature of the cancer. The notes are segmented based on clinical field labels (e.g. “IMPRESSION:”, “HISTORY:”), tab spaces, NLTK sentence tokenization [52]. To remove noise, we remove clinical field labels and



two sentences from the beginning and end of each document. We also remove sentences with common locations (e.g. “Stanford Medical Center”, “Palo Alto”) and medical doctor names (e.g. “xx xx, M.D.”) as these are often prefix or suffix to note documents. To avoid including conditions patients do not have, we remove sentences if they contain less than 15 words including a negation term (i.e. “no”, “denies”, “does not”, “none”). For example, this prevents us from extracting “smoking” as a covariate from “No history of smoking.”

We then identify biomedical entities from the preprocessed clinical notes with scispaCy [53]. scispaCy is a spaCy [54] based model for processing biomedical, scientific, and clinical text. The scispaCy models identifies a list of all the entities in the text that exist in a biomedical dictionary, such as the Unified Medical Language System [55]. We then lemmatize and combine all biomedical entities identified from the sentences for each patient into a single document. For lemmatization, we used the scispaCy lemmatizer, which is based on the spaCy lemmatization model. To further remove noise, we remove stop words using a combination of the NLTK stopwords [52] and data-specific stopwords such as medical units (e.g., “lb”, “oz”, “mmhg”), time terms (e.g., “months”, “days”), and medical or Stanford specific terms (e.g., “stanford”, “patient”, “doctor”) that are very common but irrelevant to the task at hand. We also create a dictionary of synonyms in the dataset and use the dictionary to combine these words. The dictionary includes lexical variations that are not reduced to the same root during lemmatization (e.g. “abnormality” → “abnormal”, “consult” → “consultation”), abbreviations (e.g. “hx” → “history”, “fu” → “followup”), and common synonyms (e.g. “assistance” → “service”, “action” → “movement”). Please see a list of the synonyms included in the Appendix.

Finally, we remove punctuation and generate term frequency representations of the text using bag-of-words (BOW) with term frequency–inverse document frequency (TF-IDF) weighting [56]. Bag-of-words (BOW) model is a simplifying representation in natural

language processing. It represents text (such as sentence or document) as a vector of word occurrence count. TF-IDF, is a score that reweighs the BOW matrix to reflect how important a word is to a document in a collection or corpus. We implement this with scikit-learn [49]. For prostate cancer, we select for the top 500 most frequent features using only unigrams. For NSCLC, we select for the top 1000 most frequent features using both unigrams and bigrams, and apply a document frequency threshold strictly lower than 0.7 to filter out dataset-specific stopwords. Although there are more prostate cancer patients, the lower number of death events makes it more difficult to include as many covariates when performing survival analysis. Hence, we have 500 unstructured covariates for prostate cancer and 1000 unstructured covariates for NSCLC.

We scale and normalize both the structured and unstructured covariates before concatenating them. In total, we build 509 covariates for prostate cancer and 1007 covariates for NSCLC. These covariates are then used to uncover potential dataset-specific confounders.

#### 4.4 Outcomes

We define our survival outcome as  $(Y_i, E_i)$ , where  $Y_i \in \mathbb{Z}^+$  is the number of survival days since the diagnosis and  $E_i \in \{0, 1\}$  is an indicator for whether a death event has been observed during follow-up. The treatment,  $W_i \in \{0, 1\}$ , is an indicator for either surgery, radiation, or monitoring, depending on the treatment group. The covariates,  $X_i$ , includes the structured dataset pulled from the EMR data and the bag-of-words matrix representation generated from EMR notes.

#### 4.5 Uncover and Evaluate Confounders

We uncover interpretable potential confounders from the covariates and evaluate the confounders we've identified with survival analysis. The approach is shown in Figure 1B.

We find the potential confounders by identifying covariates that are predictive of both treatment and survival outcome. We train prediction models for treatment ( $W_i = 1$ ) and the survival outcome ( $Y_i, E_i$ ) with Lasso [32] using glmnet [57]. Lasso is a  $L1$ -penalized linear regression that can produce coefficients for covariates that are exactly zero, and is, hence, often used for creating sparse models [58] or variable selection [15]. We select the intersection of covariates with non-zero coefficients from both the treatment and survival outcome models as potential confounders. For surgery vs. radiation and surgery vs. active monitoring for prostate cancer, we select the intersection covariates that correspond to the Lasso shrinkage penalty for the most regularized model such that the error is within one standard error of the minimum, *lambda.1se*. With radiation vs. monitoring for prostate cancer and surgery vs. radiation for stage I NSCLC, we select the intersection covariates that correspond to the shrinkage penalty that gives the minimum mean cross-validated error, *lambda.min*. The intersection terms selected are more stable with *lambda.1se*. However, we choose *lambda.min* for the latter two treatment groups because *lambda.1se* did not select any covariates from the text.

We then evaluate each of the covariate combinations with propensity score adjusted survival analysis. Propensity scores for patient  $i$  is the probability of receiving the treatment of interest,  $W_i = 1$ , given the covariates  $X_i$  [59]. Conditional on the propensity score, the distribution of observed covariates is expected to be the same in both branches of the treatment group. It is often used to reduce the effect of confounding in observational studies [59, 60]. In survival analysis, the hazard rate  $h(t|X)$  is the probability the patient will die within time  $t$  given covariates  $X$ . The HR is the ratio of the hazard rate of the two treatments. In survival outcomes analysis, the HR is interpreted as the effect on survival for choosing the treatment of interest,  $W_i = 1$ .

We use the Cox-proportional hazard (Cox-PH) model to perform survival regression

[61]. We assume the proportional hazards condition [62], which states that covariates are multiplicatively related to the hazard, e.g., a covariate may halve a subject’s hazard at any given time  $t$  while the baseline hazard may vary. Hence, the effect of covariates estimated by any proportional hazards model can be reported as the HR of the covariate.

In a Cox-PH model, the hazard rate of an individual is a linear function of their static covariates and a population-level baseline hazard that changes over time. We adjust for covariates (e.g. `struct:patient_age`, `struct:race_white`, etc.) against duration of survival and a binary variable indicating whether the outcome event has occurred. We estimate

$$h(t|X) = h_0(t) \exp \left( b_w W + \sum_{j=1}^p b_j X_j \right), \quad (1)$$

where  $p$  is the number of covariates,  $h_0(t)$  the baseline hazard,  $b_w$  the effect size of the treatment, and  $b_j$  the effect size of the  $j$ th covariate. The HR for a covariate is equal to  $e^{b_i}$ . We define the HR of the treatment as  $e^{b_w}$ . The Lasso regularization can also be applied to a Cox-PH model for variable selection.

We use 3 methods to estimate the HR:

- Nearest-Neighbor Matching on Propensity Score (**matching**) [22]: We perform nearest-neighbor propensity score matching (NNM) on selected covariates and estimate the HR on the matched population using a univariate Cox-PH model regressed on the treatment.
- Inverse Propensity of Treatment Weighting (**IPW**) [63] [22]: We estimate the HR using a univariate Cox-PH model regressed on the treatment with inverse propensity score weighting with stabilization [63]. The weights are defined as

$$w_i = W_i + (1 - W_i) \left[ \frac{e(X_i)}{1 - e(X_i)} \right] \quad (2)$$

- Multivariate Cox Proportional Hazard (`multi.coxph`) [61, 64, 7]: We estimate the HR using a multivariate regression model on the treatment and selected covariates to see how covariates interact with each other. The multivariate model is also weighted with the inverse propensity scores above to form a doubly-robust model.

All Cox-PH models are trained using the survival R package [65] with robust variance. Nearest-neighbor matching is performed using the MatchIt R package [66].

We estimate the propensity scores using logistic regression [67] with glmnet [57], stochastic gradient boosting [68] with gbm [69], and generalized random forests with grf [13]. We select the propensity score estimation method with the best overlap and covariate balance post propensity score adjustment.

We then compare the 3 methods for estimating HR using forest plots.

For each covariate in `struct+intersect`, we also show the univariate and multivariate Cox-PH model HR, 95% HR confidence interval, and  $p$ -value calculated using the Wald test from the survival R package [65]. Note that for the multivariate Cox-PH covariate analysis, we do not weight the model with the inverse propensity scores.

## 4.6 Data availability

The datasets analyzed for the study are not publicly available. We extracted the data from the Stanford Cancer Institute Research Database, the California Cancer Registry, and the Epic System. The EHR data cannot be redistributed to researchers other than those approved through the Stanford Institutional Review Board and those who have obtained

a Material Transfer Agreement. We have therefore given detailed description of our data selection and processing pipeline in the Methods section. To request access to the data, please contact Jiaming Zeng at [jiaming@alumni.stanford.edu](mailto:jiaming@alumni.stanford.edu).

#### 4.7 Code availability

Code for uncovering potential confounders after data processing are available at <https://github.com/jmzeng/interpretable-potential-confounders> [70]. A list of relevant packages used can be found in the README.

## 5

### References

- [1] Vinay Prasad, Andrae Vandross, Caitlin Toomey, Michael Cheung, Jason Rho, Steven Quinn, Satish Jacob Chacko, Durga Borkar, Victor Gall, Senthil Selvaraj, et al. A decade of reversal: an analysis of 146 contradicted medical practices. In *Mayo Clinic Proceedings*, volume 88, pages 790–798. Elsevier, 2013.
- [2] Payal D Soni, Holly E Hartman, Robert T Dess, Ahmed Abugharib, Steven G Allen, Felix Y Feng, Anthony L Zietman, Reshma Jagsi, Matthew J Schipper, and Daniel E Spratt. Comparison of population-based observational studies with randomized trials in oncology. *Journal of Clinical Oncology*, pages JCO–18, 2019.
- [3] Peter M Rothwell. External validity of randomised controlled trials: “to whom do the results of this trial apply?”. *The Lancet*, 365(9453):82–93, 2005.
- [4] Sharon H Giordano, Yong-Fang Kuo, Zhigang Duan, Gabriel N Hortobagyi, Jean Freeman, and James S Goodwin. Limits of observational data in determining outcomes

- from cancer therapy. *Cancer: Interdisciplinary International Journal of the American Cancer Society*, 112(11):2456–2466, 2008.
- [5] DH Yeh, S Tam, K Fung, SD MacNeil, J Yoo, E Winkvist, DA Palma, and AC Nichols. Transoral robotic surgery vs. radiotherapy for management of oropharyngeal squamous cell carcinoma—a systematic review of the literature. *European Journal of Surgical Oncology (EJSO)*, 41(12):1603–1614, 2015.
- [6] Anthony C Nichols, Julie Theurer, Eitan Prisman, Nancy Read, Eric Berthelet, Eric Tran, Kevin Fung, John R de Almeida, Andrew Bayley, David P Goldstein, et al. Radiotherapy versus transoral robotic surgery and neck dissection for oropharyngeal squamous cell carcinoma (orator): an open-label, phase 2, randomised trial. *The Lancet Oncology*, 20(10):1349–1359, 2019.
- [7] Christopher JD Wallis, Refik Saskin, Richard Choo, Sender Herschorn, Ronald T Kodama, Raj Satkunasivam, Prakesh S Shah, Cyril Danjoux, and Robert K Nam. Surgery versus radiotherapy for clinically-localized prostate cancer: a systematic review and meta-analysis. *European urology*, 70(1):21–30, 2016.
- [8] Freddie C Hamdy, Jenny L Donovan, J Athene Lane, Malcolm Mason, Chris Metcalfe, Peter Holding, Michael Davis, Tim J Peters, Emma L Turner, Richard M Martin, et al. 10-year outcomes after monitoring, surgery, or radiotherapy for localized prostate cancer. *New England Journal of Medicine*, 375(15):1415–1424, 2016.
- [9] Stephen B Williams, Jinhai Huo, Karim Chamie, Marc C Smaldone, Christopher D Kosarek, Justin E Fang, Leslie A Ynalvez, Simon P Kim, Karen E Hoffman, Sharon H Giordano, et al. Discerning the survival advantage among patients with prostate cancer who undergo radical prostatectomy or radiotherapy: the limitations of cancer registry data. *Cancer*, 123(9):1617–1624, 2017.

- [10] Alberto Abadie and Guido W Imbens. Bias-corrected matching estimators for average treatment effects. *Journal of Business & Economic Statistics*, 29(1):1–11, 2011.
- [11] Rajeev H Dehejia and Sadek Wahba. Propensity score-matching methods for nonexperimental causal studies. *Review of Economics and statistics*, 84(1):151–161, 2002.
- [12] Guido W Imbens and Donald B Rubin. *Causal inference in statistics, social, and biomedical sciences*. Cambridge University Press, 2015.
- [13] Susan Athey, Julie Tibshirani, Stefan Wager, et al. Generalized random forests. *The Annals of Statistics*, 47(2):1148–1178, 2019.
- [14] Victor Chernozhukov, Denis Chetverikov, Mert Demirer, Esther Duflo, Christian Hansen, Whitney Newey, and James Robins. Double/debiased machine learning for treatment and structural parameters, 2018.
- [15] Alexandre Belloni, Victor Chernozhukov, and Christian Hansen. High-dimensional methods and inference on structural and treatment effects. *Journal of Economic Perspectives*, 28(2):29–50, 2014.
- [16] Tianyu Wang, Marco Morucci, M Awan, Yameng Liu, Sudeepa Roy, Cynthia Rudin, and Alexander Volfovsky. Flame: A fast large-scale almost matching exactly approach to causal inference. *arXiv preprint arXiv:1707.06315*, 2017.
- [17] Reagan Mozer, Luke Miratrix, Aaron Russell Kaufman, and L Jason Anastasopoulos. Matching with text data: An experimental evaluation of methods for matching documents and of measuring match quality. *Political Analysis*, 28(4):445–468, 2020.
- [18] Margaret E Roberts, Brandon M Stewart, and Richard A Nielsen. Adjusting for confounding with text matching. *American Journal of Political Science*, 64(4):887–903, 2020.



- [19] Victor Veitch, Dhanya Sridhar, and David Blei. Adapting text embeddings for causal inference. In *Conference on Uncertainty in Artificial Intelligence*, pages 919–928. PMLR, 2020.
- [20] Katherine A Keith, David Jensen, and Brendan O’Connor. Text and causal inference: A review of using text to remove confounding from causal estimates. *arXiv preprint arXiv:2005.00649*, 2020.
- [21] Huzhang Mao, Liang Li, Wei Yang, and Yu Shen. On the propensity score weighting analysis with survival outcome: Estimands, estimation, and inference. *Statistics in medicine*, 37(26):3745–3763, 2018.
- [22] Peter C Austin. The use of propensity score methods with survival or time-to-event outcomes: reporting measures of effect similar to those used in randomized experiments. *Statistics in medicine*, 33(7):1242–1258, 2014.
- [23] Imon Banerjee, Michael Francis Gensheimer, Douglas J Wood, Solomon Henry, Sonya Aggarwal, Daniel T Chang, and Daniel L Rubin. Probabilistic prognostic estimates of survival in metastatic cancer patients (ppes-met) utilizing free-text clinical narratives. *Scientific reports*, 8(1):10037, 2018.
- [24] Michael F Gensheimer, A Solomon Henry, Douglas J Wood, Trevor J Hastie, Sonya Aggarwal, Sara A Dudley, Pooja Pradhan, Imon Banerjee, Eunpi Cho, Kavitha Ramchandran, et al. Automated survival prediction in metastatic cancer patients using high-dimensional electronic medical record data. *JNCI: Journal of the National Cancer Institute*, 111(6):568–574, 2019.
- [25] Xi Sheryl Zhang, Fengyi Tang, Hiroko H Dodge, Jiayu Zhou, and Fei Wang. Metapred: Meta-learning for clinical risk prediction with limited patient electronic health records.

- In *Proceedings of the 25th ACM SIGKDD International Conference on Knowledge Discovery & Data Mining*, pages 2487–2495, 2019.
- [26] Alvin Rajkomar, Eyal Oren, Kai Chen, Andrew M Dai, Nissan Hajaj, Michaela Hardt, Peter J Liu, Xiaobing Liu, Jake Marcus, Mimi Sun, et al. Scalable and accurate deep learning with electronic health records. *NPJ Digital Medicine*, 1(1):18, 2018.
- [27] Paul C Tang, Mary Ralston, Michelle Fernandez Arrigotti, Lubna Qureshi, and Justin Graham. Comparison of methodologies for calculating quality measures based on administrative data versus clinical data from an electronic health record system: implications for performance measures. *Journal of the American Medical Informatics Association*, 14(1):10–15, 2007.
- [28] Jiaming Zeng, Imon Banerjee, A Solomon Henry, Douglas J Wood, Ross D Shachter, Michael F Gensheimer, and Daniel L Rubin. Natural language processing to identify cancer treatments with electronic medical records. *JCO Clinical Cancer Informatics*, 5:379–393, 2021.
- [29] Joseph A Miccio, Wesley J Talcott, Vikram Jairam, Henry S Park, B Yu James, Michael S Leapman, Skyler B Johnson, Martin T King, Paul L Nguyen, and Benjamin H Kann. Quantifying treatment selection bias effect on survival in comparative effectiveness research: findings from low-risk prostate cancer patients. *Prostate Cancer and Prostatic Diseases*, pages 1–9, 2020.
- [30] Cynthia Rudin. Stop explaining black box machine learning models for high stakes decisions and use interpretable models instead. *Nature Machine Intelligence*, 1(5):206–215, 2019.
- [31] Miguel A Hernán and James M Robins. Causal inference: what if, 2020.

- [32] Robert Tibshirani. Regression shrinkage and selection via the lasso. *Journal of the Royal Statistical Society: Series B (Methodological)*, 58(1):267–288, 1996.
- [33] Joe Y Chang, Suresh Senan, Marinus A Paul, Reza J Mehran, Alexander V Louie, Peter Balter, Harry JM Groen, Stephen E McRae, Joachim Widder, Lei Feng, et al. Stereotactic ablative radiotherapy versus lobectomy for operable stage i non-small-cell lung cancer: a pooled analysis of two randomised trials. *The Lancet Oncology*, 16(6): 630–637, 2015.
- [34] Frank E Harrell Jr, Kerry L Lee, Robert M Califf, David B Pryor, and Robert A Rosati. Regression modelling strategies for improved prognostic prediction. *Statistics in medicine*, 3(2):143–152, 1984.
- [35] Frank E Harrell Jr, Kerry L Lee, and Daniel B Mark. Multivariable prognostic models: issues in developing models, evaluating assumptions and adequacy, and measuring and reducing errors. *Statistics in medicine*, 15(4):361–387, 1996.
- [36] Ping Yang, Kimary Kulig, Jennifer M Boland, Michele R Erickson-Johnson, Andre M Oliveira, Jason Wampfler, Aminah Jatoui, Claude Deschamps, Randolph Marks, Connie Fortner, et al. Worse disease-free survival in never-smokers with alk+ lung adenocarcinoma. *Journal of Thoracic Oncology*, 7(1):90–97, 2012.
- [37] Justin F Gainor, Anna M Varghese, Sai-Hong Ignatius Ou, Sheheryar Kabraji, Mark M Awad, Ryohei Katayama, Amanda Pawlak, Mari Mino-Kenudson, Beow Y Yeap, Gregory J Riely, et al. Alk rearrangements are mutually exclusive with mutations in egfr or kras: an analysis of 1,683 patients with non-small cell lung cancer. *Clinical cancer research*, 19(15):4273–4281, 2013.
- [38] Hyun Woo Lee, Young Sik Park, Sangshin Park, and Chang-Hoon Lee. Poor prognosis

- of nslc located in lower lobe is partly mediated by lower frequency of egfr mutations. *Scientific reports*, 10(1):1–8, 2020.
- [39] Yujin Kudo, Hisashi Saji, Yoshihisa Shimada, Masaharu Nomura, Jitsuo Usuda, Naohiro Kajiwara, Tatsuo Ohira, and Norihiko Ikeda. Do tumours located in the left lower lobe have worse outcomes in lymph node-positive non-small cell lung cancer than tumours in other lobes? *European journal of cardio-thoracic surgery*, 42(3):414–419, 2012.
- [40] Michael T Milano, Robert L Strawderman, Sriram Venigalla, Kimberly Ng, and Lois B Travis. Non-small-cell lung cancer after breast cancer: a population-based study of clinicopathologic characteristics and survival outcomes in 3529 women. *Journal of Thoracic Oncology*, 9(8):1081–1090, 2014.
- [41] Tomoya Kawaguchi, Minoru Takada, Akihito Kubo, Akihide Matsumura, Shimao Fukai, Atsuhisa Tamura, Ryusei Saito, Yosihito Maruyama, Masaaki Kawahara, and Sai-Hong Ignatius Ou. Performance status and smoking status are independent favorable prognostic factors for survival in non-small cell lung cancer: a comprehensive analysis of 26,957 patients with nslc. *Journal of Thoracic Oncology*, 5(5):620–630, 2010.
- [42] Michael J Crowther, Patrick Royston, and Mark Clements. A flexible parametric accelerated failure time model. *arXiv preprint arXiv:2006.06807*, 2020.
- [43] Parul Agarwal, Erin Moshier, Meng Ru, Nisha Ohri, Ronald Ennis, Kenneth Rosenzweig, and Madhu Mazumdar. Immortal time bias in observational studies of time-to-event outcomes: assessing effects of postmastectomy radiation therapy using the national cancer database. *Cancer Control*, 25(1):1073274818789355, 2018.

- [44] Firas Abdollah, Jan Schmitges, Maxine Sun, Claudio Jeldres, Zhe Tian, Alberto Briganti, Shahrokh F Shariat, Paul Perrotte, Francesco Montorsi, and Pierre I Karakiewicz. Comparison of mortality outcomes after radical prostatectomy versus radiotherapy in patients with localized prostate cancer: a population-based analysis. *International Journal of Urology*, 19(9):836–844, 2012.
- [45] R Joseph Babaian and Dorothy B Smith. Effect of ileal conduit on patients’ activities following radical cystectomy. *Urology*, 37(1):33–35, 1991.
- [46] Anne-Michelle Noone, Jennifer L Lund, Angela Mariotto, Kathleen Cronin, Timothy McNeel, Dennis Deapen, and Joan L Warren. Comparison of seer treatment data with medicare claims. *Medical care*, 54(9):e55, 2016.
- [47] Patrick Royston and Mahesh KB Parmar. Restricted mean survival time: an alternative to the hazard ratio for the design and analysis of randomized trials with a time-to-event outcome. *BMC medical research methodology*, 13(1):152, 2013.
- [48] Leo Breiman. Random forests. *Machine learning*, 45(1):5–32, 2001.
- [49] F. Pedregosa, G. Varoquaux, A. Gramfort, V. Michel, B. Thirion, O. Grisel, M. Blondel, P. Prettenhofer, R. Weiss, V. Dubourg, J. Vanderplas, A. Passos, D. Cournapeau, M. Brucher, M. Perrot, and E. Duchesnay. Scikit-learn: Machine learning in Python. *Journal of Machine Learning Research*, 12:2825–2830, 2011.
- [50] Wes McKinney et al. Data structures for statistical computing in python. In *Proceedings of the 9th Python in Science Conference*, volume 445, pages 51–56. Austin, TX, 2010.
- [51] Jun Li, David A Siegel, and Jessica B King. Stage-specific incidence rates and trends

- of prostate cancer by age, race, and ethnicity, united states, 2004–2014. *Annals of epidemiology*, 28(5):328–330, 2018.
- [52] Edward Loper and Steven Bird. Nltk: the natural language toolkit. *arXiv preprint cs/0205028*, 2002.
- [53] Mark Neumann, Daniel King, Iz Beltagy, and Waleed Ammar. Scispacy: Fast and robust models for biomedical natural language processing. *arXiv preprint arXiv:1902.07669*, 2019.
- [54] Matthew Honnibal and Ines Montani. spacy 2: Natural language understanding with bloom embeddings. *convolutional neural networks and incremental parsing*, 7(1), 2017.
- [55] Olivier Bodenreider. The unified medical language system (umls): integrating biomedical terminology. *Nucleic acids research*, 32(suppl.1):D267–D270, 2004.
- [56] Christopher D Manning, Hinrich Schütze, and Prabhakar Raghavan. *Introduction to information retrieval*. Cambridge university press, 2008.
- [57] Jerome Friedman, Trevor Hastie, and Robert Tibshirani. Regularization paths for generalized linear models via coordinate descent. *Journal of Statistical Software*, 33(1):1–22, 2010. URL <http://www.jstatsoft.org/v33/i01/>
- [58] Tim Hesterberg, Nam Hee Choi, Lukas Meier, Chris Fraley, et al. Least angle and 1 penalized regression: A review. *Statistics Surveys*, 2:61–93, 2008.
- [59] Paul R Rosenbaum and Donald B Rubin. The central role of the propensity score in observational studies for causal effects. *Biometrika*, 70(1):41–55, 1983.
- [60] Peter C Austin. An introduction to propensity score methods for reducing the effects of

- confounding in observational studies. *Multivariate behavioral research*, 46(3):399–424, 2011.
- [61] David R Cox. Regression models and life-tables. *Journal of the Royal Statistical Society: Series B (Methodological)*, 34(2):187–202, 1972.
- [62] Norman E Breslow. Analysis of survival data under the proportional hazards model. *International Statistical Review/Revue Internationale de Statistique*, pages 45–57, 1975.
- [63] Stephen R Cole and Miguel A Hernán. Adjusted survival curves with inverse probability weights. *Computer methods and programs in biomedicine*, 75(1):45–49, 2004.
- [64] Mike J Bradburn, Taane G Clark, Sharon B Love, and Douglas G Altman. Survival analysis part ii: multivariate data analysis—an introduction to concepts and methods. *British journal of cancer*, 89(3):431–436, 2003.
- [65] Terry Therneau. A package for survival analysis in s. r package version 2.37-7, 2014.
- [66] Daniel E. Ho, Kosuke Imai, Gary King, and Elizabeth A. Stuart. MatchIt: Nonparametric preprocessing for parametric causal inference. *Journal of Statistical Software*, 42(8):1–28, 2011. doi: 10.18637/jss.v042.i08.
- [67] Jerome Friedman, Trevor Hastie, and Rob Tibshirani. Regularization paths for generalized linear models via coordinate descent. *Journal of statistical software*, 33(1):1, 2010.
- [68] Jerome H Friedman. Stochastic gradient boosting. *Computational statistics & data analysis*, 38(4):367–378, 2002.

- [69] Greg Ridgeway. Generalized boosted models: A guide to the gbm package. *Update*, 1(1):2007, 2007.
- [70] Jiaming Zeng. `jmzeng/interpretable-potential-confounders`: Initial release, January 2022. URL <https://doi.org/10.5281/zenodo.5903953>

## 6 Acknowledgements

For data acquisition, we also thank A. Solomon Henry and Douglas Wood. We also thank Allison Koenecke for providing a basis for the code and Ruoxuan Xiong for reviewing previous versions of the paper. The research is supported by funding from the Stanford Human-Centered Artificial Intelligence Institute and Department of Management Science and Engineering. Athey thanks the Sloan Foundation and the Office of Naval Research grant ONR N00014-17-1-2131 for generous support.

## 7 Author Contributions Statement

J.Z. contributed to data acquisition, data processing, study design, methodology, implementation, interpretation of results, and drafted and revised the paper. M.F.G. contributed to the acquisition of data, study design, interpretation of results, and revised the paper draft. D.L.R. contributed to the acquisition of data, provision of computational resources, methodology, and revised the paper draft. S.A. contributed to study design, methodology, interpretation of results, and revised the paper draft. R.D.S. contributed to the acquisition of data, study design, methodology, interpretation of results, and revised the paper draft. All authors contributed to the study conception, provided feedback during the work development, and gave approval for the submission.



## 8 Competing Interests Statement

The authors declare that there are no competing interests.

## 9 Tables

Table 1: Characteristics of the localized prostate cancer patients.

Features	Treatment Groups		
	Surgery ( <i>n</i> = 988)	Radiation ( <i>n</i> = 385)	Monitoring ( <i>n</i> = 449)
Age, mean (std)	64.04 (7.8)	70.18 (7.6)	66.22 (8.2)
Race, no. (%)			
white	709 (71.8%)	221 (57.4%)	292 (65.0%)
black	32 (3.2%)	15 (3.9%)	14 (3.1%)
asian	94 (9.5%)	41 (10.6%)	42 (9.4%)
unknown	153 (15.4%)	108 (28.1%)	101 (22.5%)
Ethnicity, no. (%)			
hispanic	71 (7.1%)	20 (5.2%)	23 (5.1%)
non-hispanic	890 (90.1%)	348 (90.4%)	393 (87.5%)
unknown	27 (2.7%)	17 (4.4%)	33 (7.3%)
Clinical Stage, no. (%)			
stage I	219 (22.2%)	36 (9.4%)	227 (50.6%)
stage II	750 (75.9%)	289 (75.1%)	217 (48.3%)
stage III	12 (1.2%)	38 (9.9%)	3 (0.7%)
stage IV	7 (0.7%)	22 (5.7%)	2 (0.4%)
Tumor Grade, no. (%)			
grade 1	66 (66.8%)	33 (8.6%)	157 (35.0%)
grade 2	429 (43.4%)	132 (34.3%)	205 (45.7%)
grade 3	474 (48.0%)	208 (54.0%)	62 (13.8%)
grade 4	3 (0.3%)	2 (0.5%)	0 (0%)
unknown	16 (1.6%)	10 (2.6%)	25 (5.6%)
No. notes/patient, mean (std)	24.96 (44.4)	53.93 (105.7)	54.48 (93.4)
Days of survival, mean (std)	1,564.90 (979.4)	1424.76 (1,031.6)	1,403.72 (921.2)
Death, no. (%)	70 (7.1%)	19 (4.9%)	17 (3.8%)

Diagnosis Year: 2008-2017; Avg. follow up: 4.11 years

Table 2: Characteristics of the stage I lung cancer patients.

Features	Treatment Groups	
	Surgery ( <i>n</i> = 484)	Radiation ( <i>n</i> = 224)
Age, mean (std)	68.05 (10.7)	74.60 (9.1)
Gender, no. (%)		
female	299 (62.0%)	87 (41.2%)
male	185 (38.0%)	137 (58.8%)
Race, no. (%)		
white	293 (60.8%)	152 (66.5%)
black	12 (2.2%)	5 (3.5%)
asian and pacific islander	99 (20.1%)	18 (9.7%)
unknown	80 (16.9%)	49 (20.2%)
Ethnicity, no. (%)		
hispanic	23 (4.9%)	10 (3.9%)
non-hispanic	411 (84.3%)	178 (81.7%)
unknown	50 (10.8%)	36 (14.4%)
No. notes/patient, mean (std)	57.49 (101.2)	57.73 (134.9)
Days of survival, mean (std)	2,060.13 (1,207.5)	1,350.29 (914.1)
Death, no. (%)	120 (24.8%)	126 (53.3%)

Diagnosis Year: 2000-2017; Avg. follow up: 4.96 years

Table 3: Univariate and multivariate covariate-specific HR for surgery vs. radiation for prostate cancer. The \* denotes intersection terms identified by our method. The lower block of covariates represent terms extracted from clinical notes. For each covariate, we show the effect size (HR), the 95% confidence interval (CI), and the statistical significance ( $p$ -value) from a Wald statistics test.

Covariates	Univariate analysis			Multivariate analysis		
	HR	95% CI	$p$ -value	HR	95% CI	$p$ -value
W.surgery	1.27	[0.77, 2.1]	0.352	1.09	[0.59, 2]	0.777
struct:patient_age*	594.88	[87, 4.1e+03]	<0.001	35.96	[3.5, 3.7e+02]	0.003
struct:race_white	0.92	[0.44, 1.9]	0.822	0.65	[0.22, 1.9]	0.439
struct:race_api	0.63	[0.18, 2.2]	0.467	0.67	[0.14, 3.3]	0.622
struct:race_black	1.63	[0.33, 8.1]	0.551	4.04	[0.64, 25]	0.137
struct:hispanic	0.85	[0.2, 3.6]	0.831	1.52	[0.33, 7]	0.593
struct:clinical_stage	0.30	[0.042, 2.2]	0.237	1.02	[0.14, 7.4]	0.987
struct:tumor_grade	0.05	[0.0013, 2]	0.111	0.10	[0.00038, 24]	0.406
struct:grade_unknown	0.55	[0.028, 11]	0.698	0.99	[0.0029, 3.4e+02]	0.996
struct:diagnosis_year	0.12	[0.024, 0.57]	0.008	0.17	[0.025, 1.2]	0.075
text:bladder*	207.51	[79, 5.4e+02]	<0.001	35.95	[9.3, 1.4e+02]	<0.001
text:urothelial*	1919.54	[4.2e+02, 8.7e+03]	<0.001	44.07	[4.4, 4.4e+02]	0.001

HR = Hazard Ratio; CI = confidence interval; \*: intersection terms

Table 4: Univariate and multivariate covariate-specific HR for surgery vs. active monitoring for prostate cancer. The \* denotes intersection terms identified by our method. The lower block of covariates represent terms extracted from clinical notes. For each covariate, we show the effect size (HR), the 95% confidence interval (CI), and the statistical significance ( $p$ -value) from a Wald statistics test.

Covariates	Univariate analysis			Multivariate analysis		
	HR	95% CI	$p$ -value	HR	95% CI	$p$ -value
W.surgery	1.67	[0.99, 2.8]	0.057	1.02	[0.55, 1.9]	0.957
struct:patient_age*	3669.74	[5.3e+02, 2.5e+04]	<0.001	143.94	[11, 1.9e+03]	<0.001
struct:race_white	0.87	[0.41, 1.8]	0.709	0.68	[0.23, 2]	0.478
struct:race_api	0.59	[0.15, 2.3]	0.443	0.81	[0.16, 4.1]	0.799
struct:race_black	2.04	[0.41, 10]	0.384	5.16	[0.82, 32]	0.080
struct:hispanic	1.09	[0.29, 4.1]	0.898	1.68	[0.41, 6.8]	0.471
struct:clinical_stage	2.58	[0.31, 21]	0.378	3.75	[0.35, 40]	0.275
struct:tumor_grade	0.22	[0.014, 3.7]	0.296	2.37	[0.0084, 6.6e+02]	0.764
struct:grade_unknown	0.06	[0.00094, 4.2]	0.198	0.02	[2.5e-05, 14]	0.235
struct:diagnosis_year	0.12	[0.027, 0.55]	0.006	0.50	[0.073, 3.4]	0.483
text:bladder*	160.34	[65, 3.9e+02]	<0.001	24.17	[6.6, 89]	<0.001
text:urothelial*	2178.75	[5e+02, 9.6e+03]	<0.001	68.15	[7.4, 6.3e+02]	<0.001

HR = Hazard Ratio; CI = confidence interval; \*: intersection terms

Table 5: Univariate and multivariate covariate-specific HR for radiation vs. active monitoring for prostate cancer. The \* denotes intersection terms identified by our method. The lower block of covariates represent terms extracted from clinical notes. For each covariate, we show the effect size (HR), the 95% confidence interval (CI), and the statistical significance ( $p$ -value) from a Wald statistics test.

Covariates	Univariate analysis			Multivariate analysis		
	HR	95% CI	$p$ -value	HR	95% CI	$p$ -value
W.radiation	1.22	[0.63, 2.4]	0.551	0.62	[0.24, 1.6]	0.316
struct:patient_age*	265.19	[9.1, 7.8e+03]	0.001	275.03	[3.7, 2.1e+04]	0.011
struct:race_white	0.43	[0.15, 1.3]	0.129	0.39	[0.099, 1.5]	0.170
struct:race_api	1.38	[0.29, 6.7]	0.687	0.62	[0.09, 4.3]	0.626
struct:race_black	1.69	[0.18, 16]	0.646	1.90	[0.19, 19]	0.582
struct:hispanic	0.38	[0.014, 11]	0.572	0.39	[0.016, 9.7]	0.567
struct:clinical_stage	2.42	[0.2, 30]	0.491	1.12	[0.056, 22]	0.939
struct:tumor_grade	0.89	[0.034, 23]	0.942	533.75	[0.015, 1.9e+07]	0.240
struct:grade_unknown	0.12	[0.0017, 8.9]	0.337	0.00	[3e-07, 32]	0.220
struct:diagnosis_year	0.69	[0.053, 9.1]	0.781	4.96	[0.1, 2.4e+02]	0.417
text:carotid*	44.60	[4.1, 4.9e+02]	0.002	9.63	[2.1, 43]	0.003
text:resident*	185839.25	[80, 4.3e+08]	0.002	1288062.91	[1e+03, 1.6e+09]	<0.001

HR = Hazard Ratio; CI = confidence interval; \*: intersection terms

Table 6: Univariate and multivariate covariate-specific HR for surgery vs. radiation for stage I NSCLC. The \* denotes intersection terms identified by our method. The lower block of covariates represent terms extracted from clinical notes. For each covariate, we show the effect size (HR), the 95% confidence interval (CI), and the statistical significance ( $p$ -value) from a Wald statistics test.

Covariates	Univariate analysis			Multivariate analysis		
	HR	95% CI	$p$ -value	HR	95% CI	$p$ -value
W.surgery	0.309	[0.24, 0.4]	<0.001	0.545	[0.41, 0.72]	<0.001
struct:pat_age	52.9	[17, 1.6e+02]	<0.001	14.6	[4.8, 44]	<0.001
struct:male	3.07	[1.8, 5.1]	<0.001	1.92	[1.1, 3.4]	0.023
struct:race_white	0.842	[0.53, 1.4]	0.476	0.495	[0.28, 0.87]	0.015
struct:race_api	0.0557	[0.019, 0.17]	<0.001	0.0674	[0.021, 0.22]	<0.001
struct:race_black	2.03	[0.62, 6.7]	0.245	1.87	[0.57, 6.1]	0.298
struct:hispanic	0.664	[0.19, 2.3]	0.514	0.331	[0.088, 1.2]	0.101
struct:diagnosis_year	0.0166	[0.007, 0.039]	<0.001	0.0421	[0.014, 0.13]	<0.001
text:alert	9.46e-12	[3.6e-16, 2.5e-07]	<0.001	0.00224	[3e-08, 1.7e+02]	0.287
text:alk	1.17e+04	[38, 3.7e+06]	0.001	4.67e+04	[9.3e+02, 2.3e+06]	<0.001
text:appearance	5.46e-09	[2.6e-12, 1.1e-05]	<0.001	0.00694	[7.6e-06, 6.4]	0.153
text:attention	1.03e-12	[4.6e-20, 2.3e-05]	0.001	0.00238	[1.2e-09, 4.7e+03]	0.414
text:feel	6.64e-10	[5.7e-16, 0.00077]	0.003	1.27e-05	[1.2e-10, 1.4]	0.057
text:left.low	29.1	[5.2, 1.6e+02]	<0.001	12.5	[2.1, 76]	0.006
text:nipple	2.57e-09	[1.6e-15, 0.0041]	0.007	4.2e-05	[1.5e-09, 1.2]	0.054
text:rib	688	[40, 1.2e+04]	<0.001	28.1	[1.8, 4.4e+02]	0.017
text:severe	601	[56, 6.5e+03]	<0.001	58.3	[9.4, 3.6e+02]	<0.001
text:sponge	2.04e-07	[3.3e-11, 0.0013]	<0.001	0.0181	[3.7e-05, 8.9]	0.205
text:squamous.cell	94.8	[16, 5.6e+02]	<0.001	7.61	[1.1, 53]	0.041
text:venous	0.0464	[0.00089, 2.4]	0.128	0.0523	[0.00081, 3.4]	0.165

HR = Hazard Ratio; CI = confidence interval; \*: intersection terms

## 10 Figure Legends/Captions



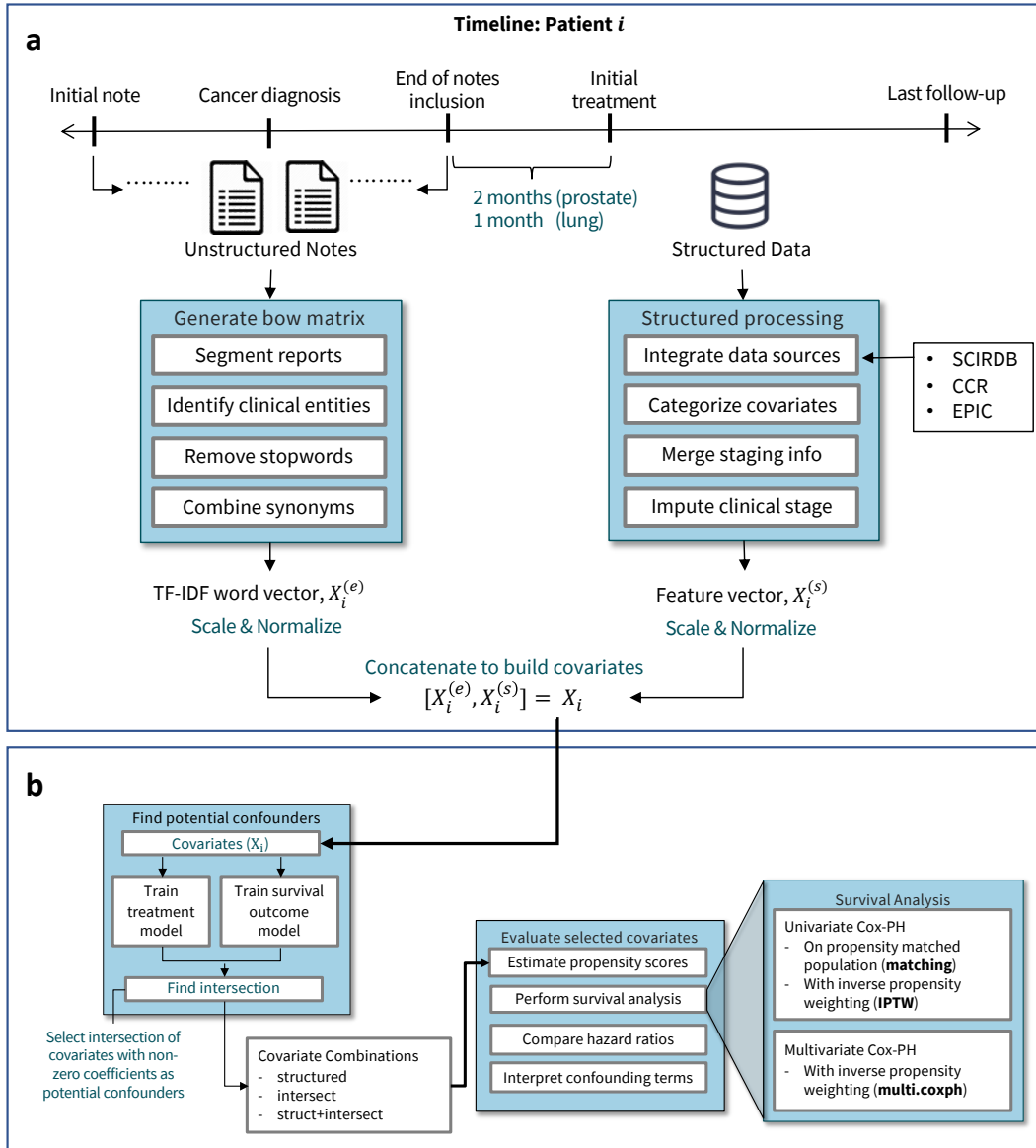


Figure 1: Pictorial overview for uncovering potential confounders. **1a** shows the data processing done for each patient. We preprocess and concatenate the structured and unstructured covariates before applying our method. For the data sources, we compile data from the Stanford Cancer Institute Research Database (SCIRDB), the California Cancer Registry (CCR), and the Epic System. We present the timeline for patient  $i$  with both structured ( $X_i^{(s)}$ ) and unstructured ( $X_i^{(e)}$ ) features  $X_i$ . **1b** shows the workflow for identifying how potential confounders affect survival analysis for each treatment group. We uncover covariates that are predictive of both the treatment and outcome as potential confounders. We then perform survival analysis on different combinations of the selected covariates.



Figure 2: For each treatment group, we show the unpenalized coefficients for the struct+intersect covariates. Blue text indicates the intersect covariates that have been selected as potential confounders by our method from the text; the prefix text: has been omitted. Black text indicates the structured covariates that have not been selected; the prefix “struct:” has been omitted. The covariate patient\_age has been shorthand as pat.age. For the treatment model, these are the coefficients to a linear model. For the survival outcome model, these are the  $\beta$  for the Cox-PH model. The dotted lines are the axis, denote a coefficient value of 0. We plot the coefficients from the survival and treatment regression models in each of the figure panels: [2a](#)) surgery vs. radiation for prostate cancer; [2b](#)) surgery vs. monitoring for prostate cancer; [2c](#)) surgery vs. monitoring for prostate cancer; [2d](#)) surgery vs. radiation for NSCLC.

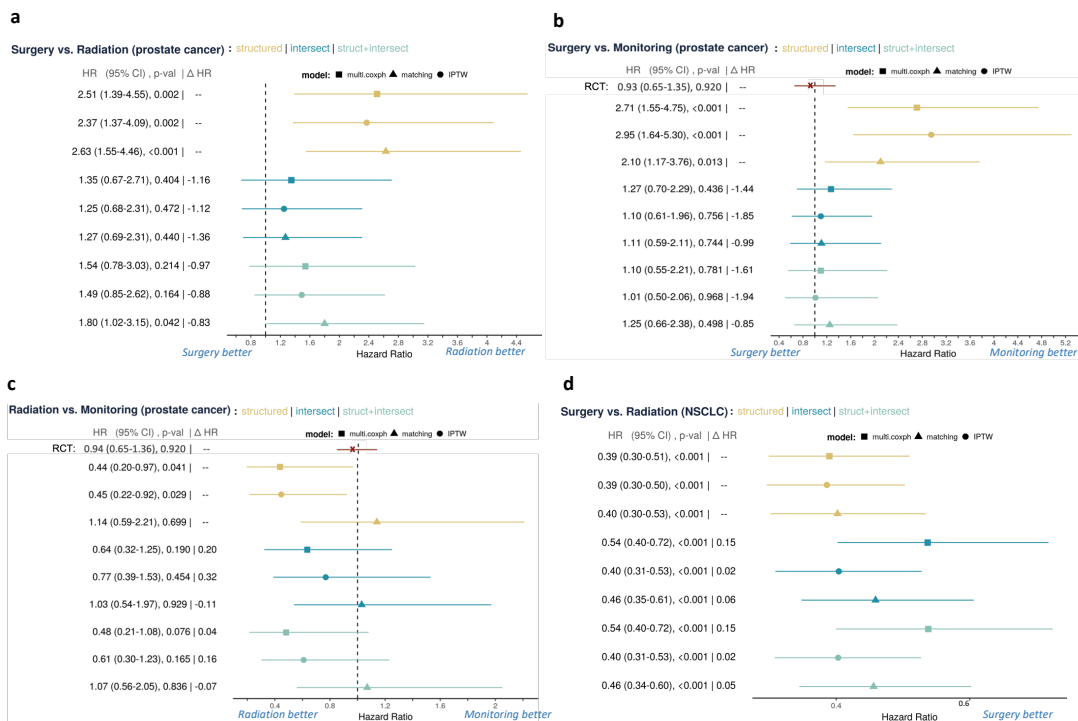


Figure 3: Forest plots of each of the comparison groups. The left-hand label displays the mean HR, the 95% confidence interval (CI), the  $p$ -value, and the  $\Delta$  HR. The  $\Delta$  HR measure is the difference of the current HR estimate and the baseline, structured, HR estimate. For surgery vs. active monitoring and radiation vs. active monitoring for prostate cancer, we've included the exact results from the RCT in red for comparison. For the remaining cohorts, clinical expertise suggest equipose between the treatments. We see that the inclusion of our potential confounders shift the HR point estimate in the direction of the RCT and reduces the selection bias. The blue labels below each graph indicate which treatment is better in terms of HR comparison. We display the HR comparisons for each cohort as following: **3a**) surgery vs. radiation for prostate cancer; **3b**) surgery vs. monitoring for prostate cancer; **3c**) surgery vs. monitoring for prostate cancer; **3d**) surgery vs. radiation for NSCLC. For **3d**, "Radiation better" is not displayed because the HR value is not shifted beyond 1.0, the direction of radiation better.

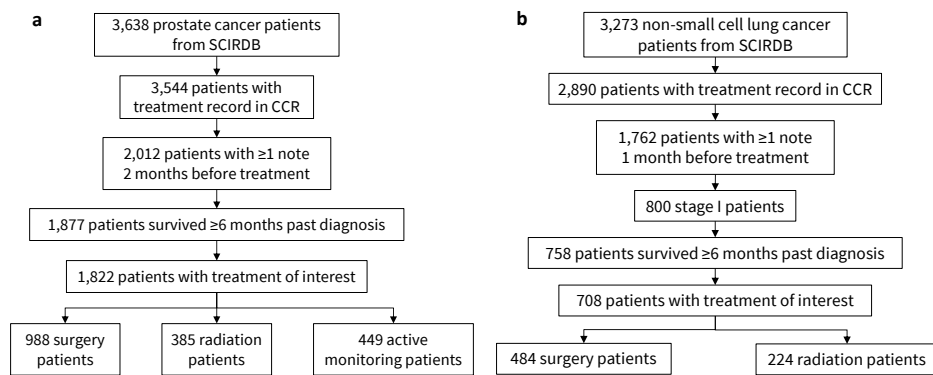


Figure 4: Patient cohort selection process for prostate and lung cancer patients. In 4a, we show the cohort filtering process the the subsequent number of patients selected for prostate cancer. In 4b, we show the filtering process for NSCLC.

## Supplementary Information

### 1 Supplementary: Glossary of Structured Covariates

Supplementary Table I shows a glossary of the structured features extracted from the EMRs.

Supplementary Table 1: Glossary of structured features extracted from EMR data. The types of variables include: binary (B), categorical(C), and continuous (CT).

	Feature	Type	Description
Demographic	race_white	B	1 if patient identifies as race white
	race_black	B	1 if patient identifies as race black
	race_api	B	1 if patient identifies as race asian or pacific islander
	hispanic	B	1 if patient identifies as hispanic
	nonhispanic	B	1 if patient identifies as nonhispanic
	patient_age	C	age split into 7 categories
Cancer Description	clinical_stage	C	clinical stage categories
	tumor_grade	C	tumor grade categories
	grade_unknown	B	1 if patient grade is unknown
	diagnosis_year	CT	year initial diagnosis is recorded

### 2 Supplementary: Dictionary of Synonyms

We used a dictionary of synonyms based on a list of the most common words to reduce noise in our dataset. Please see the list of synonyms below:

- {“abnormality” → “abnormal”, “admission” → “admit”, “assistance” → “assistant”, “bilateral” → “bilaterally”, “bleeding” → “bleed”, “consult” → “consultation”, “diagnostic” → “diagnosis”, “evaluate” → “evaluation”, “hx” → “history”, “functional”

→ “function”, “fu” → “followup”, “gentleman” → “man”, “disease” → “illness”,  
“imaging” → “image”, “improvement” → “improve”, “invasion” → “invasive”, “ac-  
tion” → “movement”, “neurologic” → “neurological”, “operative” → “operation”,  
“polyps” → “polyp”, “postop” → “postoperative”, “pulse” → “rate”, “reaction” →  
“reactive”, “refer” → “referral”, “removal” → “remove”, “resp” → “respiratory”,  
“smoke” → “smoking”, “assistance” → “service”, “spinal” → “spine”, “surgical” →  
“surgery”, “assessment” → “test”, “testing” → “test”, “therapeutic” → “therapy”,  
“treat” → “treatment”, “visualize” → “visual”}

### 3 Supplementary: Confounders

Confounding is a major challenge when estimating causal effect from observational studies. The structure of confounding can be represented by causal diagrams. In Supplementary Figure [1](#) we present a series of Directed Acyclic Graphs (DAGs) that show different causal structures with potential confounding, based on the examples in Hernán and Robins [\[31\]](#), Chapter 7. In the following diagrams, we define  $Y$  as the outcome,  $W$  as the treatment, and  $X$  as the covariate that has been identified as a potential confounder.

Supplementary Figure [1a](#) shows the most natural case of confounding. Treatment  $W$  is a cause of outcome  $Y$  and confounder  $X$  is a cause of both  $W$  and  $Y$ . Therefore, the association between  $W$  and  $Y$  includes both the direct causal effect and an indirect “backdoor” path from  $W$  to  $Y$  through  $X$ . Conditioning on the confounder  $X$  blocks this second path, allowing the accurate estimation of the causal effect of  $W$  on  $Y$ . Examples of this type of confounder include fixed patient characteristics such as a patient’s age or cancer clinical stage. For example, older patients can have worse survival outcomes, so doctors might assign different treatments to older patients; cancer patients with higher clinical stage can also have worse survival outcomes, affecting doctors’ treatment decisions.

Our method is designed to uncover and adjust for this type of confounder, as is appropriate.

Supplementary Figure 1b and 1c show different structures where  $W$  is a cause of  $Y$ , where  $X$  is a cause of one and associated with the other through an unmeasured cause  $U$ . In these cases, conditioning on confounder  $X$  blocks the “backdoor” path between  $W$  and  $Y$ ; in such cases, conditioning on  $X$  is necessary to avoid bias in estimating the causal effect of  $W$  on  $Y$ , since part of the correlation between  $X$  and  $Y$  arises due to the relationship between ( $U$ ) and both  $W$  and  $Y$ . Confounding of type 1b can arise when  $U$  represents a type of lung cancer mutation. Even if a mutation test is not performed (and so the mutation is unobserved), the mutation ( $U$ ) affects the symptoms recorded in the notes ( $X$ ), as well as the patient outcomes ( $Y$ ). An example of 1b uncovered from our NSCLC study is `text:left.low`, tumor location on the left lower lobe. Location of cancer ( $X$ ) directly effects treatment decisions, and EGFR mutated lung cancer ( $U$ ) is less likely to be positioned in the lower lobe [38]. For these examples, conditioning on the text describing the cancer location is appropriate, and is necessary if the backdoor path is not blocked by other covariates  $X$ .

Supplementary Figure 1d shows a structure where  $W$  is a cause of  $Y$ , and  $X$  is a cause of neither of them. In 1d, conditioning on  $X$  will not eliminate the backdoor path between  $W$  and  $Y$ , but it might reduce its effect. Confounding of type 1d may arise when  $U$  represents patient “performance status” (a measure of how the disease impacts the patient’s daily living abilities), which is not typically recorded in the patient’s chart as a structured field, but can directly effect both treatment decision and survival outcome [41]. Some examples of 1d uncovered from our NSCLC study include `text:discomfort`, `text:alert`, and `text:attention`.

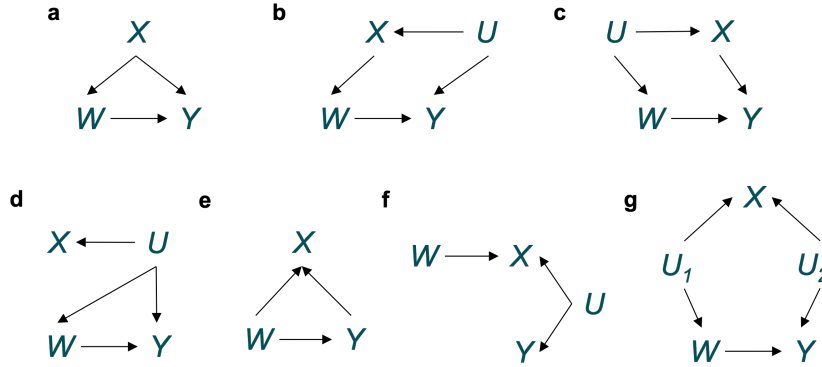
Supplementary Figure 1e shows a structure where  $W$  is a cause of  $X$ , but not a cause of  $Y$ . In such cases, conditioning on  $X$  introduces a backdoor path between  $W$  and  $Y$ .

Confounding of the type shown in [1e](#) can arise when  $X$  represents short-term effects post treatment and  $U$  represents patient health status. Our study design avoids such cases by only considering pre-treatment covariates.

Supplementary Figure [1f](#) shows a structure where  $W$  and  $Y$  are causes of  $X$ . In this case, the covariate  $X$  is referred to as a collider, and conditioning on  $X$  introduces a backdoor path between  $W$  and  $Y$ . Our study design also avoids such cases by only considering pre-treatment covariates.

Supplementary Figure [1g](#) show another structure where  $W$  is a cause of  $Y$ , and  $X$  is a cause of neither of them. Unlike [1d](#), conditioning on  $X$  in [1g](#) opens a backdoor path between  $W$  and  $Y$ , introducing bias into the causal estimate of the effect of  $W$  on  $Y$ . Situations such as [1g](#) are a potential limitation of our methodology, but in some cases they can be recognized through inspection and reasoning. Examples of [1g](#) are words selected in earlier iterations of our study such as text:menlo, referring to the location Menlo Park, CA. A patient's education level ( $U_1$ ) can effect both their treatment preference and also their living location; a patient's socioeconomic status ( $U_2$ ) can effect their survival outcome and living location. Although text:menlo is associated with treatment and outcome through  $U_1$  and  $U_2$ , treating it as a confounder would introduce bias. We were able to filter out some of these terms by selecting only biomedical-related terms. Clinical expertise is needed to avoid scenario [1g](#).





Supplementary Figure 1: Causal diagrams showing different potential cases of confounders. For the diagrams,  $X$  represents the features;  $Y$  represents the outcome;  $W$  represents the treatment; and  $U, U_1, U_2$  are potential unknown confounders.

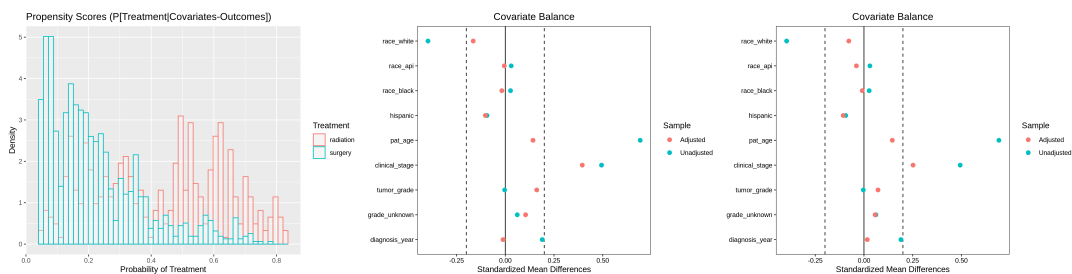
## 4 Supplementary: Propensity Score and Covariate Balance

### Plots

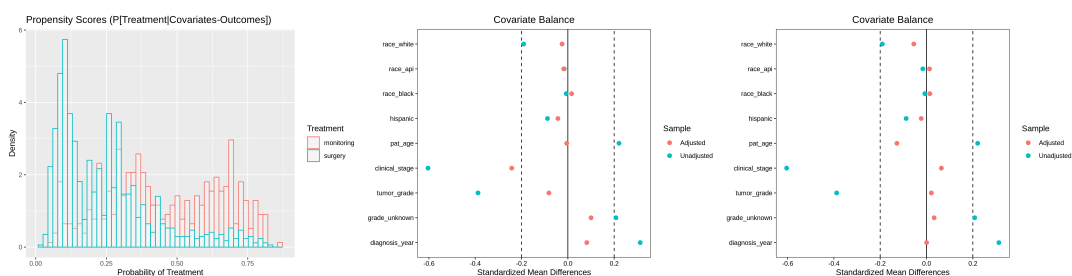
We show the propensity scores and covariate balance plots for each of the results plotted in Figure 3 of the main paper. In Supplementary Figure 2, we show the plots for *structured*. In Supplementary Figure 3, we show the plots for *intersect*. In Supplementary Figure 4, we show the plots for *struct+intersect*.

## 5 Supplementary: Covariate Correlation

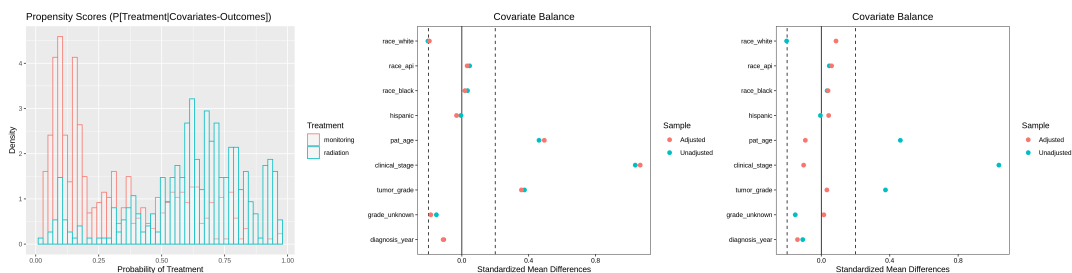
We show the  $R^2$  values for all combinations of the selected covariates for each of the treatment groups. The  $R^2$  is the square of the correlation from linear regression. It measures the proportion of variation in the dependent variable that can be attributed to the independent variable. In Supplementary Table 2, we show the  $R^2$  values for surgery vs. radiation for prostate cancer. In Supplementary Table 3, we show the  $R^2$  values for surgery vs. monitoring for prostate cancer. In Supplementary Table 4, we show the  $R^2$  values for



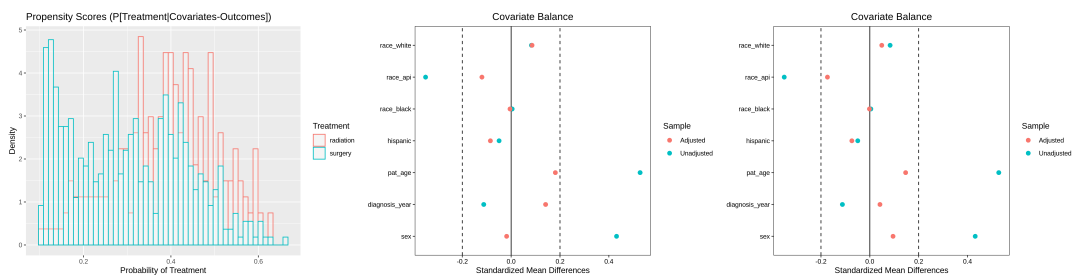
(a) Surgery vs Radiation (prostate, grf)



(b) Surgery vs Monitoring (prostate, glmnet)

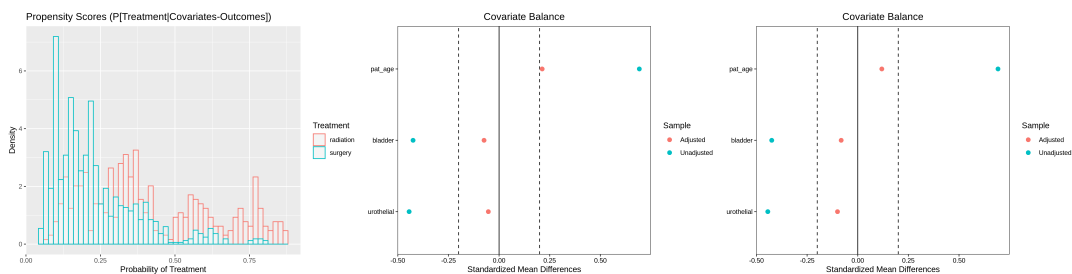


(c) Monitoring vs Radiation (prostate, glmnet)

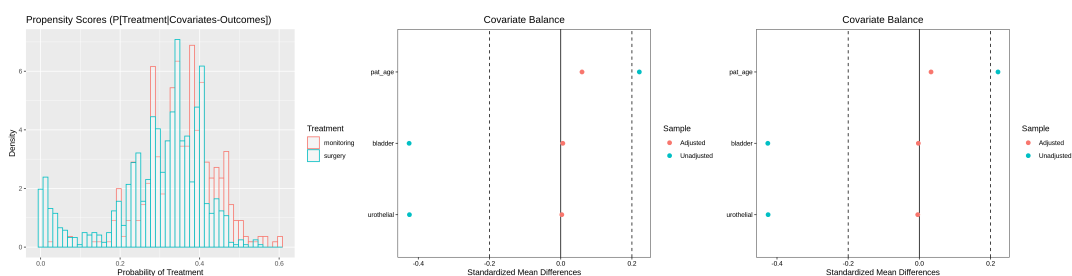


(d) Surgery vs Radiation (lung, grf)

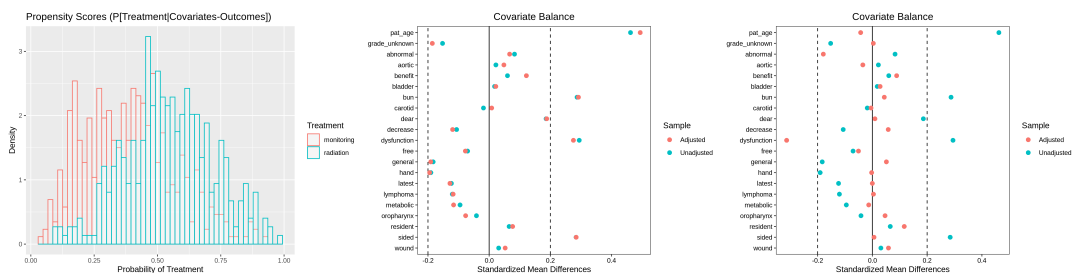
Supplementary Figure 2: Supplementary plots to the structured results presented in Figure 3 (left) Propensity score plot with structured. (middle) Covariate balance plot for matching. (right) Covariate balance plots for IPTW.



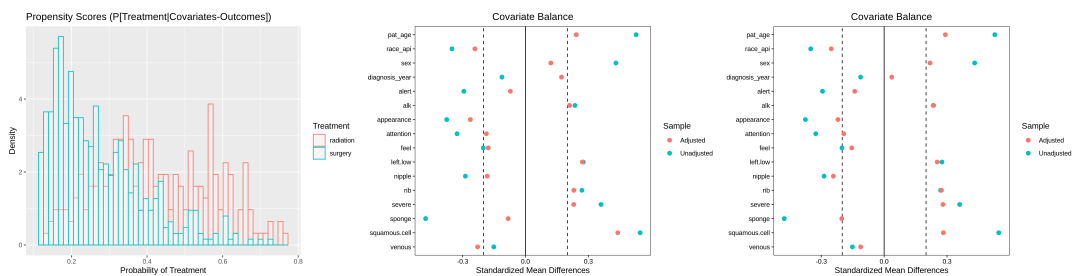
(a) Surgery vs Radiation (prostate, grf)



(b) Surgery vs Monitoring (prostate, glmnet)

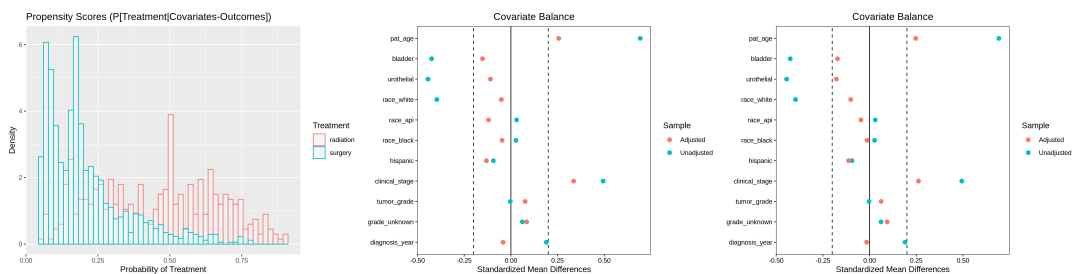


(c) Monitoring vs Radiation (prostate, glmnet)

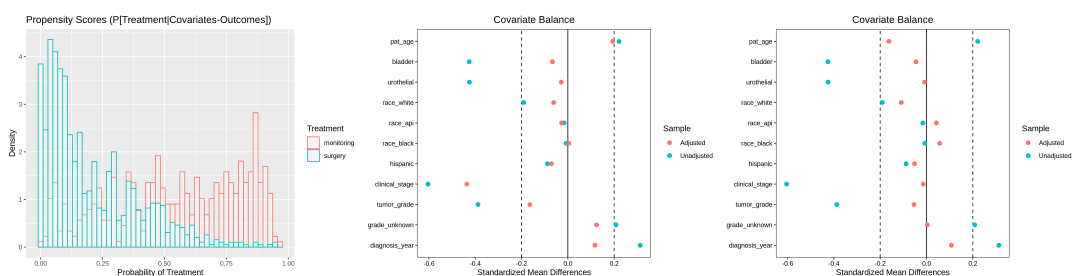


(d) Surgery vs Radiation (lung, grf)

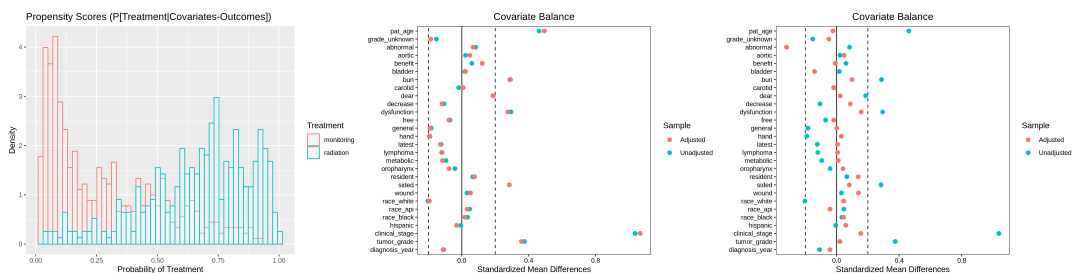
Supplementary Figure 3: Supplementary plots to the intersect results presented in Figure 3 (left) Propensity score plot with intersect. (middle) Covariate balance plot for matching. (right) Covariate balance plots for IPTW.



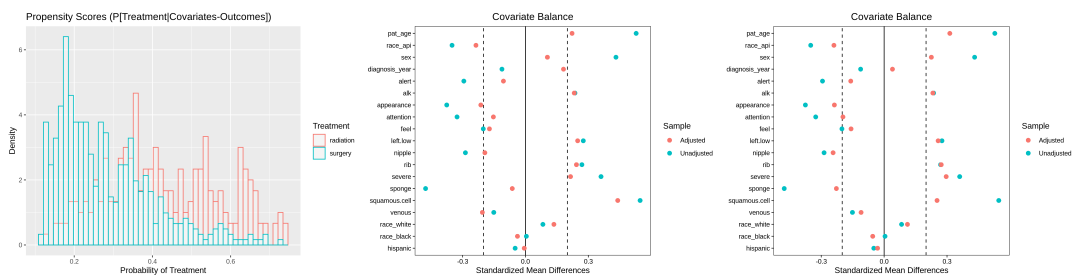
(a) Surgery vs Radiation (prostate, grf)



(b) Surgery vs Monitoring (prostate, glmnet)



(c) Monitoring vs Radiation (prostate, glmnet)



(d) Surgery vs Radiation (lung, grf)

Supplementary Figure 4: Supplementary plots to the struct+intersect results presented in Figure 3. (left) Propensity score plot with struct+intersect. (middle) Covariate balance plot for matching. (right) Covariate balance plots for IPTW.

radiation vs. monitoring for prostate cancer. In Supplementary Table 5, we show the  $R^2$  values for surgery vs. radiation for NSCLC.

Supplementary Table 2:  $R^2$  correlation of the struct+intersect covariates of surgery vs. radiation for prostate cancer.

	struct:patient_age	text:bladder	text:urothelial	struct:race_white	struct:race_api	struct:race_black	struct:hispanic	struct:clinical_stage	struct:tumor_grade	struct:grade_unknown	struct:diagnosis_year
struct:patient_age	0.04	0.01	0.00	0.00	0.00	0.00	0.01	0.00	0.00	0.00	0.02
text:bladder	0.04	0.47	0.01	0.00	0.00	0.00	0.00	0.04	0.03	0.00	0.00
text:urothelial	0.01	0.47	0.01	0.00	0.00	0.00	0.00	0.04	0.03	0.00	0.00
struct:race_white	0.00	0.01	0.01	0.22	0.00	0.07	0.05	0.00	0.00	0.00	0.03
struct:race_api	0.00	0.00	0.00	0.22	0.00	0.00	0.01	0.00	0.00	0.00	0.00
struct:race_black	0.00	0.00	0.00	0.07	0.00	0.00	0.00	0.00	0.00	0.00	0.00
struct:hispanic	0.01	0.00	0.00	0.05	0.01	0.00	0.00	0.00	0.00	0.00	0.00
struct:clinical_stage	0.00	0.04	0.04	0.00	0.00	0.00	0.00	0.04	0.04	0.01	0.03
struct:tumor_grade	0.00	0.03	0.03	0.00	0.00	0.00	0.00	0.04	0.51	0.51	0.21
struct:grade_unknown	0.00	0.00	0.00	0.00	0.00	0.00	0.00	0.01	0.51	0.51	0.02
struct:diagnosis_year	0.02	0.00	0.00	0.03	0.00	0.00	0.00	0.03	0.21	0.21	0.02

Supplementary Table 3:  $R^2$  correlation of the struct+intersect covariates of surgery vs. monitoring for prostate cancer.

	struct:patient_age	text:carotid	text:resident	struct:race_white	struct:race_api	struct:race_black	struct:hispanic	struct:clinical_stage	struct:tumor_grade	struct:grade_unknown	struct:diagnosis_year
struct:patient_age	0.02	0.00	0.00	0.00	0.01	0.01	0.00	0.04	0.01	0.01	0.07
text:carotid	0.02	0.00	0.00	0.00	0.00	0.00	0.00	0.00	0.01	0.00	0.00
text:resident	0.00	0.00	0.00	0.00	0.00	0.01	0.00	0.00	0.00	0.00	0.00
struct:race_white	0.00	0.00	0.00	0.17	0.17	0.06	0.02	0.00	0.00	0.00	0.00
struct:race_api	0.01	0.00	0.00	0.17	0.00	0.00	0.00	0.00	0.00	0.00	0.01
struct:race_black	0.01	0.00	0.01	0.06	0.00	0.00	0.00	0.00	0.00	0.00	0.00
struct:hispanic	0.00	0.00	0.00	0.02	0.00	0.00	0.00	0.00	0.00	0.00	0.00
struct:clinical_stage	0.04	0.00	0.00	0.00	0.00	0.00	0.00	0.05	0.05	0.01	0.06
struct:tumor_grade	0.01	0.01	0.00	0.00	0.00	0.00	0.00	0.05	0.66	0.66	0.22
struct:grade_unknown	0.01	0.00	0.00	0.00	0.00	0.00	0.00	0.01	0.66	0.66	0.04
struct:diagnosis_year	0.07	0.00	0.00	0.00	0.01	0.00	0.00	0.06	0.22	0.22	0.04

Supplementary Table 4:  $R^2$  correlation of the struct+intersect covariates of radiation vs. monitoring for prostate cancer.

	struct:patient_age	text:cavotid	text:resident	struct:race_white	struct:race_api	struct:race_black	struct:hispanic	struct:clinical_stage	struct:tumor_grade	struct:grade_unknown	struct:diagnosis_year
struct:patient_age											
text:cavotid	0.02		0.00	0.00	0.01	0.01	0.00	0.04	0.01	0.01	0.07
text:resident	0.00	0.00		0.00	0.00	0.00	0.00	0.00	0.01	0.00	0.00
struct:race_white	0.00	0.00	0.00		0.00	0.01	0.00	0.00	0.00	0.00	0.00
struct:race_api	0.01	0.00	0.00	0.17		0.06	0.02	0.00	0.00	0.00	0.00
struct:race_black	0.01	0.00	0.01	0.06	0.00		0.00	0.00	0.00	0.00	0.01
struct:hispanic	0.00	0.00	0.00	0.02	0.00	0.00		0.00	0.00	0.00	0.00
struct:clinical_stage	0.04	0.00	0.00	0.00	0.00	0.00	0.00		0.00	0.00	0.00
struct:tumor_grade	0.01	0.01	0.00	0.00	0.00	0.00	0.00	0.05		0.01	0.06
struct:grade_unknown	0.01	0.00	0.00	0.00	0.00	0.00	0.00	0.01	0.66		0.22
struct:diagnosis_year	0.07	0.00	0.00	0.00	0.01	0.00	0.00	0.06	0.22	0.04	

Supplementary Table 5:  $R^2$  correlation of the struct+intersect covariates of surgery vs. radiation for NSCLC. Due to the size of the table, we've omitted the "struct:" and "text:" prefixes for the covariates.

	patient_age	race_api	sex	diagnosis_year	alert	alk	allergy	appearance	attention	cyst	discomfort	eye	fever	inginal	nipple	rib	severe	silhouette	sponge	squamous	racc.white	race.black	hispanic
patient_age	0.00	0.01		0.04	0.01	0.00	0.00	0.02	0.01	0.00	0.01	0.00	0.00	0.00	0.00	0.00	0.01	0.00	0.01	0.00	0.00	0.00	0.00
race_api	0.00		0.00	0.03	0.02	0.00	0.00	0.03	0.00	0.00	0.00	0.00	0.00	0.01	0.00	0.01	0.00	0.00	0.00	0.01	0.30	0.00	0.01
sex	0.01	0.00		0.04	0.01	0.01	0.01	0.01	0.01	0.02	0.00	0.01	0.00	0.02	0.02	0.00	0.00	0.00	0.01	0.01	0.02	0.00	0.00
diagnosis_year	0.04	0.03	0.04		0.11	0.01	0.03	0.02	0.01	0.00	0.00	0.01	0.01	0.01	0.00	0.01	0.00	0.00	0.01	0.01	0.01	0.00	0.00
alert	0.01	0.02	0.01	0.11		0.00	0.02	0.04	0.01	0.00	0.00	0.01	0.01	0.05	0.00	0.00	0.00	0.00	0.02	0.00	0.00	0.00	0.00
alk	0.00	0.00	0.01	0.01	0.00		0.00	0.00	0.00	0.00	0.00	0.00	0.00	0.00	0.00	0.00	0.01	0.00	0.00	0.00	0.00	0.00	0.00
allergy	0.00	0.00	0.01	0.03	0.02	0.00		0.02	0.00	0.00	0.00	0.00	0.01	0.04	0.00	0.02	0.00	0.00	0.00	0.00	0.00	0.00	0.00
appearance	0.02	0.03	0.01	0.02	0.04	0.00	0.02		0.00	0.00	0.00	0.00	0.03	0.00	0.00	0.00	0.00	0.00	0.00	0.00	0.00	0.00	0.00
attention	0.01	0.00	0.01	0.01	0.01	0.00	0.00	0.00		0.00	0.00	0.00	0.00	0.00	0.00	0.00	0.00	0.00	0.00	0.00	0.00	0.00	0.00
cyst	0.00	0.00	0.02	0.00	0.00	0.00	0.00	0.00	0.00		0.00	0.00	0.00	0.00	0.00	0.01	0.00	0.00	0.00	0.00	0.00	0.00	0.00
discomfort	0.01	0.00	0.00	0.00	0.01	0.00	0.00	0.00	0.00	0.00	0.00	0.00	0.00	0.00	0.00	0.01	0.01	0.00	0.00	0.00	0.01	0.00	0.00
eye	0.00	0.00	0.01	0.00	0.01	0.00	0.01	0.00	0.00	0.00	0.00	0.00	0.00	0.00	0.00	0.00	0.00	0.00	0.00	0.00	0.00	0.00	0.00
fever	0.00	0.00	0.00	0.01	0.05	0.00	0.04	0.03	0.00	0.00	0.00	0.00	0.00	0.01	0.00	0.00	0.00	0.00	0.00	0.00	0.00	0.00	0.00
inginal	0.00	0.01	0.02	0.01	0.00	0.00	0.00	0.00	0.00	0.00	0.00	0.00	0.01	0.00	0.00	0.00	0.00	0.00	0.00	0.01	0.00	0.00	0.00
nipple	0.00	0.00	0.02	0.00	0.00	0.00	0.02	0.00	0.00	0.01	0.00	0.00	0.00	0.00	0.00	0.00	0.00	0.00	0.00	0.00	0.01	0.00	0.00
rib	0.00	0.01	0.00	0.01	0.00	0.00	0.00	0.00	0.00	0.00	0.01	0.00	0.01	0.00	0.00	0.00	0.00	0.00	0.00	0.00	0.00	0.00	0.00
severe	0.01	0.00	0.00	0.00	0.00	0.01	0.00	0.00	0.00	0.00	0.01	0.00	0.00	0.00	0.00	0.00	0.00	0.00	0.01	0.00	0.00	0.00	0.01
silhouette	0.00	0.00	0.00	0.00	0.00	0.00	0.00	0.00	0.00	0.00	0.00	0.00	0.00	0.00	0.00	0.00	0.00	0.00	0.00	0.00	0.00	0.00	0.00
sponge	0.01	0.00	0.01	0.01	0.02	0.00	0.00	0.00	0.00	0.00	0.00	0.00	0.00	0.00	0.00	0.00	0.01	0.00	0.00	0.00	0.00	0.00	0.00
squamous	0.00	0.01	0.01	0.01	0.00	0.00	0.00	0.00	0.00	0.00	0.00	0.00	0.00	0.01	0.00	0.00	0.00	0.00	0.00	0.00	0.01	0.00	0.00
race.white	0.00	0.30	0.02	0.01	0.00	0.00	0.00	0.00	0.00	0.01	0.00	0.00	0.00	0.00	0.01	0.00	0.00	0.00	0.01	0.00	0.00	0.04	0.04
race.black	0.00	0.00	0.00	0.00	0.00	0.00	0.00	0.00	0.00	0.00	0.00	0.00	0.00	0.00	0.00	0.00	0.00	0.00	0.00	0.00	0.04	0.00	0.00
hispanic	0.00	0.01	0.00	0.00	0.00	0.00	0.00	0.00	0.00	0.00	0.00	0.00	0.00	0.00	0.00	0.01	0.01	0.00	0.00	0.00	0.04	0.00	0.00